THE ASTROPHYSICAL JOURNAL, 412:771–791, 1993 August 1

WHAT ARE THE MASS-LOSS RATES OF O STARS?

HENNY J. G. L. M. LAMERS[1,2] AND CLAUS LEITHERER[3,4]
Received 1992 October 12; accepted 1993 February 9

ABSTRACT

Empirical mass-loss rates of 28 luminous galactic OB stars are derived from thermal radio emission and from Hα recombination radiation. The velocity fields of all stars had previously been analyzed in the *IUE* ultraviolet spectral region. The results of these ultraviolet line-profile analyses (shape of the velocity law and terminal velocity) are combined with the radio and Hα data for a precise and consistent determination of the stellar mass-loss rates. It is found that radio and Hα rates agree within the observational errors. This suggests that significant clumping in the wind is unlikely due to the very different radius of origin of radio and Hα radiation within the wind.

Comparison of the empirical mass-loss rates with values derived theoretically from the theory of radiatively driven winds demonstrates that theoretical mass-loss rates are *lower* on the average by 0.29 dex. Similarly, theoretical terminal velocities are *higher* by 40%. By combining the observed wind velocities with the mass-loss rates we show that the empirical momentum fluxes are also *higher* by 0.17 dex than the prediction of the theory. The theoretical momentum fluxes are independent of the stellar masses. Therefore the momentum (and also the mass-loss and terminal velocity) discrepancy cannot be explained by systematic errors in the adopted stellar masses.

We find that the discrepancy between theoretical and empirical mass-loss rates increases with increasing wind density. By including a sample of WNL stars with weak winds in our sample, we show that the most luminous O stars form a natural extension of the least extreme WNL stars with respect to the momentum transfer rate to the stellar winds. It is suggested that the "momentum problem" observed in Wolf-Rayet stars is already present in a less severe form in luminous O stars. This can provide an explanation for the mass-loss and terminal velocity discrepancy in hot stars.

Subject headings: radio continuum: stars — stars: early-type — stars: mass loss

1. INTRODUCTION

Recent studies of the stellar winds of O stars have shown that there is a discrepancy of about 40% between the measured and the predicted terminal velocities of the winds. The empirical values of v_∞, derived from the P Cygni profiles of the UV resonance lines by detailed line fitting by Groenewegen, Lamers, & Pauldrach (1989), are about 40% smaller than those predicted by the radiation-driven wind models (Kudritzki, Pauldrach, & Puls 1987; Pauldrach et al. 1990; Kudritzki et al. 1991). This discrepancy was also found by Blomme (1990). Groenewegen et al. (1989) have argued that there are two possible explanations for this discrepancy: either the most sophisticated stellar wind models which include 10^5 lines from 136 ions are still inadequate or the stellar parameters which were adopted from theoretical stellar evolution tracks are systematically wrong.

1. *If* the predictions of the stellar wind theory are quantitatively correct, the fact that the observed values of v_∞ are lower than predicted by about 40% implies that the escape velocities, v_{esc}, of the O stars at their photospheres are smaller than predicted from evolutionary models by about 40%, because v_∞ is approximately proportional to v_{esc}. A reduction of v_{esc} by about 40% for O stars requires a reduction of the stellar mass, M, derived from the luminosity, L, and temperature, T_{eff}, by about 40% even in the main-sequence phase. There is no simple explanation for such a large error in the predicted mass-luminosity relation of massive stars with $M \gtrsim 30\ M_\odot$.

2. On the other hand, *if* the discrepancy between predicted and observed terminal velocities is due to errors in the radiation-driven wind models, this also has important consequences. If the radiation-driven wind theory predicts too high terminal velocities it is likely to predict too low mass-loss rates, if the amount of momentum transferred from the radiation into the wind is correct. If the mass-loss rates predicted by the radiation-driven wind theory were used in stellar evolution calculations, the errors in the mass-loss rates would result in serious errors in the predicted evolutionary tracks.

Kudritzki et al. (1992) have argued that the predictions of the radiation-driven wind theory for O stars could in principle provide a very powerful method to derive stellar parameters (T_{eff}, M, and even the distance). Such a method for determining distances would be extremely valuable, since O stars are very luminous and can presently be observed in the UV up to the distance of M31 (Hutchings et al. 1992).

In view of the importance of the accurate predictions of the radiation-driven wind model, we decided to make a careful comparison between the observed values of v_∞ and $\dot{M}$ of O stars and the values predicted by the radiation-driven wind theory. In a first-order approximation one might expect that models which overestimate the terminal velocity of the winds will underestimate the mass-loss rates since their product depends on the momentum of the radiation transferred into

[1] SRON Laboratory for Space Research, Sorbonnelaan 2, 3584 CA Utrecht, The Netherlands.
[2] Astronomical Institute, University of Utrecht, Princetonplein 5, Utrecht, The Netherlands.
[3] Space Telescope Science Institute, 3700 San Martin Drive, Baltimore, MD 21218, which is operated by the Association of Universities for Research in Astronomy, Inc., under contract with NASA.
[4] Affiliated with the Astrophysics Division of the Space Science Department of ESA.

the wind. This check might give information on the possible source of the discrepancies.

The same problem was recently addressed in a study by Herrero et al. (1992). These authors compared the observed terminal velocities of the winds of O stars with those predicted by the radiation-driven wind theory by using stellar parameters, $T_{\rm eff}$ and log g, that were derived from the photospheric spectrum. They showed that the predictions agree with the observations *if* the spectroscopic masses are adopted. However, these spectroscopic masses are on the average considerably lower than the masses derived from the evolutionary tracks. This suggests that there is a problem with the method of determining the spectroscopic gravities of O stars if the evolutionary masses can be shown to be correct. Vice versa, if spectroscopic gravities are correct, a severe problem in our understanding of massive star evolution exists.

In this study we will adopt the stellar parameters derived from stellar evolutionary tracks. Subsequently we will discuss how different choices of the stellar masses would affect the derived stellar-wind parameters.

We will consider only the most reliable determinations of the mass-loss rates, i.e., those derived from the free-free emission of the wind at radio wavelengths, and those derived from the emission of Hα in the wind. The mass-loss rates derived from the free-free emission in the infrared (IR) are not very reliable because they depend on the accurate knowledge of the photospheric continuum in the IR and on the density structure (or velocity law) in the upper photosphere or the lower part of the wind. Both effects are not accurately known (see, e.g., Lamers 1988). Although Hα also samples the inner regions of the stellar wind, it is less sensitive to those effects than the infrared free-free emission. The mass-loss rates derived from the UV resonance lines are not very reliable because the lines which are the best empirical indicators of mass loss in early-type stars (N V at 1240 Å, C IV at 1550 Å, and Si IV at 1400 Å) are from ions whose degree of ionization in O stars cannot be accurately predicted by the presently available theoretical stellar wind models. Groenewegen & Lamers (1991) have shown that the predicted and observed ionization fractions in the winds of O stars can differ by as much as a factor of 10 or more.

In § 2 we will select a number of O stars with reasonably accurately determined mass-loss rates. In § 3 we discuss the mass-loss rates of these stars derived from radio emission. The mass-loss rates derived from Hα are discussed in § 4. Radio and Hα mass-loss rates are compared in § 5. In § 6 we give the mass-loss rates which are predicted by the radiation-driven wind models of the Munich group, Kudritzki and colleagues, based on a simple but accurate algorithm derived by Kudritzki et al. (1989). The observed and predicted mass-loss rates and terminal wind velocities are compared. In § 7 we discuss the possible origin of the discrepancies between predictions and observations. In § 8 we will discuss the consequences of the results for evolution of massive stars. Finally, § 9 highlights the main results.

2. THE PROGRAM STARS

The stars used in this study are listed Table 1. They were selected on the basis of four criteria: (i) accurate determinations of v_∞ from UV line profiles; (ii) measured free-free emission at radio or mm wavelengths; (iii) measured upper limit for the radio or mm flux if this gives a significant upper limit for the mass-loss rate; (iv) reliable measurement of the

TABLE 1

PARAMETERS OF THE PROGRAM STARS

HD	Name	Spectral Type		T_{eff}	BC	M_V	log L	D	M	R	ϵ	Γ	log g_{eff}	v_{esc}	v_∞	$\frac{v_\infty}{v_{esc}}$
		Garmany	Walborn	$[10^3 K]$			$[L_\odot]$	$[kpc]$	$[M_\odot]$	$[R_\odot]$				$[km\ s^{-1}]$	$[km\ s^{-1}]$	
14947		O5 f	O5 If$^+$	40.3	3.78	−6.10	5.86	2.3	52	17	0.15	0.34	3.51	880	2300 ± 70	2.61
15558		O5 III	O5 III(f)	42.3	3.92	−6.40	6.02	2.2	68	19	0.15	0.38	3.51	930	3350 ± 200	3.60
15570		O4 I	O4 If$^+$	42.4	3.93	−6.70	6.14	2.2	79	22	0.15	0.43	3.41	890	2600	2.92
15629		O5 V	O5 V ((f))	44.3	4.06	−5.50	5.74	2.2	51	13	0.10	0.28	3.78	1040	2900 ± 70	2.79
24912	ξ Per	O7.5 III	O7.5 III(n)(f)	37.1	3.55	−5.10	5.38	0.4	31	12	0.18	0.18	3.68	890	2400 ± 100	2.70
30614	α Cam	O9.5 I	O9.5 Ia	30.9	3.04	−6.70	5.78	1.1	43	27	0.15	0.32	3.04	640	1550 ± 60	2.42
36486	δ Ori	O9.5 II	O9.5 II	32.9	3.22	−6.57	5.82	0.5	45	25	0.15	0.34	3.12	680	2000	2.94
36861	λ Ori	O8 III	O8 III((f))	36.0	3.46	−5.20	5.38	0.5	31	13	0.15	0.19	3.61	860	2400 ± 150	2.79
37043	ι Ori	O9 III	O9 III	34.0	3.31	−5.90	5.58	0.5	36	18	0.15	0.24	3.36	760	2450 ± 150	3.22
37128	ε Ori	B0 Ia	B0 Ia	28.0	2.75	−7.00	5.80	0.5	42	34	0.20	0.29	2.85	580	1500 ± 150	2.59
37742	ζ Ori	O9.5 I	O9.7 Ib	30.9	3.04	−7.00	5.90	0.5	49	31	0.15	0.37	2.95	620	2100 ± 150	3.39
46150		O5 V	O5 V((f))	44.3	4.06	−5.50	5.74	1.5	51	13	0.09	0.29	3.77	1030	2900 ± 200	2.82
46223		O4 V	O4 V((f))	46.4	4.21	−5.30	5.70	1.5	52	11	0.10	0.25	3.95	1170	2800 ± 60	2.39
47839	15 Mon	O7 V	O7 V((f))	40.1	3.78	−4.80	5.34	0.7	33	10	0.07	0.18	3.89	1020	2300 ± 200	2.25
57061		O9 II	O9 II	34.0	3.31	−7.00	6.02	1.5	61	29	0.15	0.39	3.09	700	1960	2.80
66811	ζ Pup	O4 I	O4 I(n)f	42.4	3.93	−6.06	5.90	0.4	59	16	0.17	0.32	3.63	970	2200 ± 60	2.27
93129A		O3 I	O3 If*	50.5	4.12	−7.00	6.35	3.5	125	20	0.09	0.47	3.66	1130	3050 ± 60	2.70
149038	μ Nor	O9.5 I	O9.7 Iab	30.9	3.04	−6.70	5.78	1.3	43	27	0.15	0.32	3.04	640	1750 ± 100	2.73
149404		O9 I	O9 Ia	32.0	3.14	−7.24	6.05	1.4	61	34	0.15	0.42	2.92	630	2450	3.89
149757	ζ Oph	O9 V	O9.5 V	35.9	3.46	−4.30	5.00	0.1	24	8	0.16	0.10	3.94	990	1500 :	1.52:
151804		O8 I	O8 Iaf	34.0	3.31	−7.30	6.14	1.9	69	34	0.15	0.46	2.94	640	1600 ± 70	2.50
152408		O8 I	O8: Iafpe	34.0	3.31	−7.00	6.02	1.9	60	29	0.15	0.40	3.07	690	960 :	1.38:
152424		O9.5 I	OC9.7 Ia	30.9	3.04	−7.10	5.94	1.9	52	33	0.15	0.38	2.91	610	1760	2.89
164794	9 Sgr	O4 V	O4 V((f))	46.4	4.21	−6.10	6.02	1.6	72	16	0.10	0.38	3.68	1030	2950 ± 150	2.86
188001	9 Sge	O8 I	O7.5 Iaf	34.0	3.31	−6.60	5.86	2.4	49	24	0.15	0.34	3.19	720	1800 ± 70	2.50
190429A		O4 I	O4 If$^+$	42.4	3.93	−6.50	6.06	2.7	72	20	0.15	0.39	3.48	920	2300 ± 70	2.50
190864		O6.5 III	O6.5 III(f)	39.2	3.70	−5.60	5.62	2.3	41	14	0.17	0.24	3.64	920	2450 ± 150	2.66
210839	λ Cep	O6 I	O6 I(n)fp	38.2	3.62	−6.30	5.86	0.8	52	19	0.15	0.34	3.42	830	2100 ± 60	2.53

equivalent width of Hα. All program stars meet criterion (i) and at least one of the other criteria. The stars in the Cyg OB2 association that have a measured radio flux due to free-free emission were excluded because of criterion (i). Moreover, the stellar parameters of these stars are very uncertain.

Since the adopted stellar parameters are critical for this study we will discuss them in some detail. We have used the most modern set of stellar parameters. The spectral types are from the catalog of O stars from C. D. Garmany (private communication). They are based on numerous classification studies by Walborn. For comparison, we also give in Table 1 the spectral types published by Walborn (1972, 1973a, and private communication) and by Walborn & Fitzpatrick (1990). The two sets of spectral classifications are in very good agreement. Since we adopted distances from Garmany's work, we also used her spectral types, for reasons of consistency. The values of $T_{\rm eff}$ and the bolometric correction (BC) are derived from the relation between $T_{\rm eff}$ or BC and spectral type from Chlebowski & Garmany (1991). These relations are based on non–LTE studies of about a dozen stars, mainly by the Munich group (e.g., Kudritzki et al. 1991). For the star of type O3f we adopted the new determination of $T_{\rm eff} = 50{,}500$ K from Kudritzki et al. (1991) and the corresponding bolometric correction of BC = 4.12.

For the 10 stars in common with the studies of Herrero et al. (1992), Kudritzki et al. (1991), and Voels et al. (1989), our adopted values of $T_{\rm eff}$ agree with theirs within 10%, with a mean ratio of $T_{\rm eff}$(this study)/$T_{\rm eff}$(non–LTE) = 1.01 ± 0.04. The most discrepant star is HD 149757, O9 V, for which we adopted $T_{\rm eff} = 32{,}500$ K. HD 149757 is a peculiar fast rotator which recently had a shell episode (Ebbets 1981). Its effective temperature may be somewhat different from normal O stars of the same spectral type. The other O9 V star in the sample of Herrero et al. has $T_{\rm eff} = 37{,}500$ K which agrees much better with the general trend of $T_{\rm eff}$ versus spectral type. The agreement between our adopted temperatures and those derived from detailed non–LTE studies is shown in Figure 1. The stars included in this figure are HD 24912, HD 46150, HD 47839, HD 149757, HD 190864 (non–LTE $T_{\rm eff}$ values from Herrero et al. [1992]); HD 30614, HD 36486, HD 37742 (non–LTE $T_{\rm eff}$ values from Voels et al. [1989]); HD 66811, HD 93129A (non–LTE $T_{\rm eff}$ values from Kudritzki et al. [1991]).

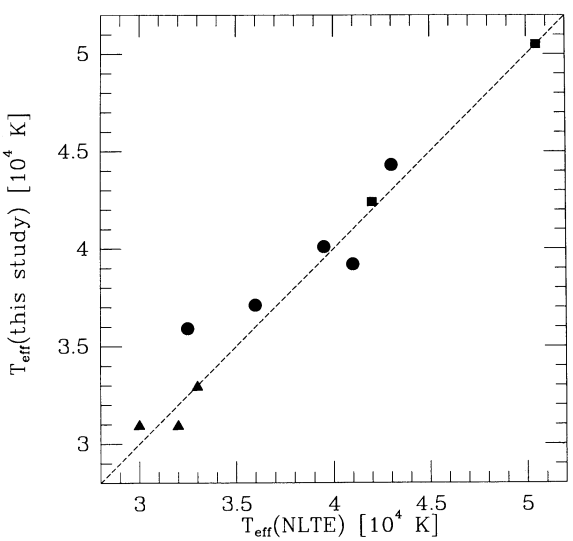

FIG. 1.—Comparison between $T_{\rm eff}$ derived from non–LTE studies and $T_{\rm eff}$ adopted here. Circles refer to non–LTE temperatures of Herrero et al. (1992); squares are based on Kudritzki et al. (1991); triangles denote values of Voels et al. (1989).

The distances and the values of M_V are also from the O-star catalog of Garmany. These distances and the values of the interstellar extinction used for M_V are largely based on the study of cluster distances from Humphreys (1978). The bolometric magnitudes are derived rom M_V and BC. These data agree very well with those adopted by Groenewegen et al. (1989) in their study of the terminal velocities of the winds. The data for the B0 supergiant ε Ori are from Groenewegen et al. (1989). We have compared the different determinations of $T_{\rm eff}$ and L, and we conclude that the accuracy of $T_{\rm eff}$ is about 0.03 dex and the accuracy of L is about 0.2 dex.

Five of our program stars are known runaway stars. Recently Blaauw (1993) has redetermined the distances of these stars on the basis of their accurate space velocities and identification of their parent cluster. The stars and their resulting values of M_V are ξ Per (−5.3), α Cam (−6.9), ζ Pup (−7.2:), ζ Oph (−4.1), and λ Cep (−6.3). Except for ζ Pup these values of M_V agree with our adopted values within 0.2 mag, which is well within the estimated accuracy of our values. For ζ Pup, Blaauw's value of M_V is 1.1 mag brighter than the value we adopted, corresponding to an increase in distance by a factor 1.7. However, the distance determination by Blaauw for this star is uncertain because of its uncertain association with a cluster. We also note that the absolute magnitudes of HD 36486 and HD 93129A have a further uncertainty due to multiplicity of these stars (Voels et al. 1989; Walborn 1973b). An additional complication arises from the relatively large reddening correction for HD 93129A ($A_V \approx 1.6$; Walborn 1973b).

The masses of the stars are derived from $T_{\rm eff}$ and L using the evolutionary tracks of Maeder (1990) which include mass loss and overshooting. The uncertainty in the masses, resulting from the uncertainty in $T_{\rm eff}$ and L is about 0.10 dex. The radius (R) was derived from L and $T_{\rm eff}$ and the gravity was derived from M and R. The accuracy of R is about 0.16 dex. The effective gravity, $g_{\rm eff}$, is defined as the Newtonian gravity corrected for the radiation pressure due to electron-scattering: $g_{\rm eff} = g(1 - \Gamma)$, where

$$\Gamma = 7.66 \times 10^{-5} \sigma_e \left(\frac{L}{L_\odot}\right)\left(\frac{M_\odot}{M}\right). \quad (1)$$

The electron scattering coefficient, σ_e, depends on the degree of ionization and on the He/H ratio. For the abundance of helium we adopted the results of the detailed non–LTE abundance analysis of O and early B stars by Kudritzki et al. (1991) and Herrero et al. (1992). These studies show that the ratio ϵ = He/(H + He) by number is 0.10 ± 0.03 for O stars of luminosity class V and $\epsilon = 0.15 \pm 0.05$ for class I, II, and III. We adopt these values, except for the stars studied by Kudritzki et al. and Herrero et al. for which we adopted their values of ϵ. The values of ϵ are listed in Table 1.

The values of σ_e depend on the abundance of helium and on the degree of ionization near the critical point at the bottom of the wind. From the non–LTE model atmospheres calculated by Pauldrach et al. (1990) we find the following values of σ_e for O stars with $\epsilon = 0.10$:

$$\sigma_e = 0.34 \text{ cm}^2 \text{ g}^{-1} \quad \text{if } T_{\rm eff} \geq 35{,}000 \text{ K},$$

$$\sigma_e = 0.32 \text{ cm}^2 \text{ g}^{-1} \quad \text{if } 30{,}000 \text{ K} \leq T_{\rm eff} < 35{,}000 \text{ K},$$

$$\sigma_e = 0.31 \text{ cm}^2 \text{ g}^{-1} \quad \text{if } T_{\rm eff} < 30{,}000 \text{ K}.$$

For other helium abundances we have scaled these values accordingly:

$$\sigma_e = 0.401 \frac{1 + q\epsilon}{1 + 3\epsilon}, \quad (2)$$

where q is the fraction of He^{++} and $1 - q$ is the fraction of He^{+}, with $q = 1$ if $T_{\rm eff} \geq 35{,}000$ K, $q = 1/2$ if 30,000 K $\leq T_{\rm eff} < 35{,}000$ K, and $q = 0$ if $T_{\rm eff} < 30{,}000$ K. Notice that σ_e decreases by about 0.02 if ϵ increases from 0.10 to 0.15.

The error in Γ due to the small uncertainty in σ_e is negligible compared to the uncertainty in g. The uncertainty in Γ is about 0.13 dex because the uncertainty in L of 0.2 dex is partly compensated by the resulting uncertainty in M of 0.1 dex after taking into account the mass-luminosity relation.

The effective velocity of escape, $v_{\rm esc}$ was derived from $g_{\rm eff}$ and R. The values of $v_{\rm esc}$ have a typical uncertainty of 10% if $\Gamma \lesssim 0.3$ (i.e., for the majority of the program stars), and 28% if $\Gamma = 0.4$. The small uncertainty in $v_{\rm esc}$ for $\Gamma \lesssim 0.3$, in spite of the large uncertainty in R, is due to the fact that the errors in M and R cancel one another because $M \propto L^{0.5}$ and $R \propto L^{0.5} T_{\rm eff}^{-2}$ so that $v_{\rm esc} \propto T_{\rm eff}$. All the uncertainties mentioned above indicate the possible deviations from the values listed in Table 1 due to $\delta \log L = 0.2$ and $\delta \log T_{\rm eff} = 0.03$. These uncertainties are maximum errors and not standard deviations. The determination of the mass-loss rates requires the knowledge of the terminal velocities of the stellar winds. The terminal velocities of most of our program stars have been derived by Groenewegen et al. (1989) by means of accurate line fitting with the SEI (Sobolev Exact Integration) method. They have shown that these terminal velocities are very similar, i.e., within about 100 km s^{-1}, to those derived from line fits calculated with the Comoving Frame Code. For stars not studied by Groenewegen et al. (1989) we used the terminal velocities from Prinja, Barlow, & Howard (1990) who used several methods to derive v_∞ from the line profiles. For stars in common with Groenewegen et al. the values of v_∞ from Prinja et al. agree reasonably well, with v_∞(Prinja)/v_∞(Groenewegen) = 0.97 ± 0.11. For the five stars in common with Herrero et al. (1992) we find that v_∞(Herrero)/v_∞(Groenewegen) = 1.01 ± 0.06. The accuracy of v_∞ is estimated to be about 150 km s^{-1} for stars of class I–III, and about 300 km s^{-1} for stars of class V, which have less saturated lines.

We adopt a velocity law of the type

$$v(r) = v_0 + (v_\infty - v_0)\left(1 - \frac{R}{r}\right)^{\beta}, \quad (3)$$

where v_0 is the velocity at the base of the wind near the critical point, and β is a parameter that describes the steepness of the velocity law. This law was adopted because the analysis of the UV resonance lines by Groenewegen et al. (1989) demonstrates that it fits the observations and because the theory of radiation-driven stellar winds predicts such a law (Pauldrach, Puls, & Kudritzki 1986). Groenewegen et al. found that $\beta \approx 0.7$–0.8 for O stars, in agreement with predictions. We will adopt a mean value of $\beta = 0.70 \pm 0.10$.

3. MASS-LOSS RATES FROM THE RADIO FREE-FREE EMISSION

3.1. *The Radio Fluxes*

Among all methods to derive accurate mass-loss rates, radio measurements are considered to give the most reliable values of $\dot{M}$. Radio mass-loss rates are relatively free of uncertain assumptions and systematic effects, such as, e.g., the unknown ionization fractions of ions used to derive ultraviolet mass-loss rates. On the other hand, radio measurements of hot stars are challenging from a technical point of view due to the low flux densities of hot stars at radio wavelengths. As a consequence, only a few O stars have been measured in this wavelength regime. Most of the earlier work has been done by Abbott and collaborators, as summarized by Bieging, Abbott, & Churchwell (1989). We adopted their fluxes at 2 and 6 cm (see Table 2). Recently Howarth & Brown (1991) obtained new measurements at 3.6 cm for a significant number of O stars which had not yet been detected. Their study more than doubled the number of O stars detected at radio wavelengths, and we also included their observations in our set of data. The star HD 15558 which was detected at 3.6 cm was not included in our study of the mass-loss rates from radio data. Bieging et al. (1989) found that the radio flux was variable by about a factor 2 and concluded that it is probably a nonthermal emitter. This

TABLE 2

RADIO FLUXES OF THE PROGRAM STARS

HD	Spectral Type	$S_\nu[mJy]$				thermal
		1.3 mm	2.0 cm	3.6 cm	6.0 cm	
14947	O5 f				< 0.5	?
15570	O4 I		< 0.2	0.11 ± 0.03	< 0.2 ± 0.1	prob
30614	O9.5 I				0.35 ± 0.10	prob
36486	O9.5 II			0.30 ± 0.01		?
36861	O8 II I				< 0.19	?
37043	O9 III			0.046 ± 0.015		?
37128	B0 Ia	13.1 ± 2.2			1.6	def
37742	O9.5 I			0.89 ± 0.04	0.7	def
57061	O9 II			0.35 ± 0.03		?
66811	O4 I	20.2 ± 1.8	3.0 ± 0.2	1.60 ± 0.07	1.3 ± 0.1	def
149038	O9.5 I				< 0.24	?
149404	O9 I			0.73 ± 0.03		?
149757	O9 V			0.18 ± 0.02		?
151804	O8 I				0.4 ± 0.1	prob
152408	O8 I	14.7 ± 3.1	2.4 ± 0.1		1.1 ± 0.1	def
152424	O9.5 I			0.21 ± 0.04		?
210839	O6 I			0.38 ± 0.03		?

agrees with the flux of 0.53 ± 0.03 mJy measured at 3.6 cm by Howarth & Brown which indicates a spectral index of about 0 if the highest observed flux of 0.5 mJy at 6 cm is adopted. The fluxes at 1.3 mm are from Leitherer & Robert (1991). All fluxes are listed in Table 2. We indicate in this table whether the radio flux is definitely (def) or probably (prob) due to free-free emission. This information is derived from the slope for the spectrum and from the absence of polarization (see Bieging et al. 1989; Leitherer & Robert 1991). Several objects have "?" listed in column (7) of Table 2, indicating that nothing is known about a possible nonthermal contribution to the observed radio flux. Comparison with the observed Hα emission (see below) suggests that none of these stars exhibits significant nonthermal emission at cm wavelengths. We mention that HD 149404 shows very strong Hα emission, which is consistent with the mass-loss rates associated with the strong 3.6 cm flux.

3.2. *Determination of the Mass-Loss Rates*

The free-free emission in the radio wavelength region from an ionized stellar wind originates from large distances (typically 10^1–10^3 R) because the free-free opacity increases with wavelength as λ^2. At such large distances the wind has already reached its terminal velocity so that the density varies as r^{-2}. This allows an analytic solution to the equation of radiative transfer (Panagia & Felli 1975; Wright & Barlow 1975). In this case the mass-loss rate is related to the observed radio flux as

$$S_\nu = 2.32 \times 10^4 \left(\frac{\dot{M} Z}{v_\infty \mu}\right)^{4/3} (\gamma g_\nu \nu)^{2/3} D^{-2}, \quad (4)$$

where μ is the mean weight per ion, Z is the rms ionic charge, γ is the ratio of electron to ion density, ν is the frequency, g_ν is the Gaunt factor, D is the distance in kpc, and S_ν is the flux in mJy. The Gaunt factor can be approximated by

$$g_\nu = 9.77\left(1 + 0.13 \log \frac{T_e^{3/2}}{Z\nu}\right), \quad (5)$$

where T_e is the electron temperature of the wind at the distance $r \gtrsim 10$–100 R where the radio flux originates (Abbott et al. 1986). Since the Gaunt factor is approximately proportional to $\nu^{-0.15}$ in the radio region, the free-free radio flux of an ionized wind is expected to vary approximately as $\nu^{0.6}$.

For the calculation of the Gaunt factor we assumed an electron temperature at $r \gtrsim 100$ R of $T_e = 0.5 T_{\rm eff}$. This assumption is supported by calculations of the radiative equilibrium in stellar winds (Drew 1989), which include the effects of adiabatic cooling and radiative loses due in metallic lines and the heating and cooling in the continua of H and He. The calculations suggest that T_e is $0.5 T_{\rm eff}$ or less at $r > 10$ R. We notice that the mass-loss rates derived from the radio fluxes depend only weakly on T_e through g_ν. Relation (4) is valid only if the radio flux is thermal, i.e. $S_\nu \propto \nu^{0.6}$, and does not contain a nonthermal component. This can be checked by measuring the radio flux at at least two wavelengths. We will use only the radio fluxes of stars that are definite or probable free-free emitters. The mass-loss rates derived from the radio flux depend on abundances (via μ) and on the degree of ionization. Hydrogen will be fully ionized in the winds of O stars, but helium can be singly or doubly ionized. This will affect the values of Z and γ. For this purpose we have calcuated the ionization structure of the winds of O stars with the non–LTE code of de Koter, Schmutz, & Lamers (1993), in which the equations of radiative transfer and the statistical equilibrium are solved simultaneously. The H and He^+ atom are represented by five-level atoms. For neutral helium we adopted a 13-level atom with 78 transitions in non–LTE. For details, see de Koter et al. (1993). The density structure was calculated from the equation of mass continuity and the velocity law of equation (3) with $\beta = 0.7$. We assumed an initial velocity of v_0 equal to the sound speed at the sonic point. The temperature was calculated in the gray approximation of a spherically expanding wind with a lower limit of $0.5 T_{\rm eff}$ (see Wessolowski, Schmutz, & Hamann 1988). The results of these calculations will be described by Lamers & de Koter (1993). They found that H is fully ionized in the winds of O stars, as expected, and that helium is singly or doubly ionized. For a given distance (r) in the wind ionization of He depends on $T_{\rm eff}$ and on the density structure of the wind, but hardly on the temperature structure or on the abundance of He. This can be expressed in a simple way: He is mainly He^+ at a distance r if $T_{\rm eff} < T_{\rm rec}(r)$ and He^{++} if $T_{\rm eff} \geq T_{\rm rec}(r)$, where $T_{\rm rec}(r)$ is the value of $T_{\rm eff}$ for which the wind recombines from He^{++} to He^+ at a distance r. $T_{\rm rec}(r)$ depends on the density in the wind. We define a characteristic density as

$$\langle \rho \rangle = \frac{\dot{M}}{4\pi R^2 v_\infty}. \quad (6)$$

For the velocity law of equation (3) with $\beta = 0.7$ we find that $\langle \rho \rangle = \rho(1.5R)$ and $0.41\langle \rho \rangle = \rho(2R)$. The values of $T_{\rm rec}$ at $r = 10$ R and 100 R are listed in Table 3 for various values of $\langle \rho \rangle = 3.6 \times 10^{-14}$ g cm^{-3} He is doubly ionized at $r = 10$ R if $T_{\rm eff} > 35{,}500$ K and doubly ionized at $r = 100$ R if $T_{\rm eff} > 36{,}250$ K. For stars with 35,500 K $< T_{\rm eff} <$ 36,250 K He^{++} recombines to He^+ at a distance between 10 and 100 R. We can approximate these results with a simple quadratic equation

$$\log T_{\rm rec}(10\ R) = 13.449 + 1.267 \log \langle \rho \rangle + 0.045(\log \langle \rho \rangle)^2, \quad (7)$$

$$\log T_{\rm rec}(100\ R) = 13.539 + 1.273 \log \langle \rho \rangle + 0.045(\log \langle \rho \rangle)^2. \quad (8)$$

Notice that these temperatures are strongly dependent on $\langle \rho \rangle$. This implies that stars of the same temperature can have different degrees of ionization if the densities in their wind are different. The data in Table 3 show that helium can be He^{++} in the winds of stars with $T_{\rm eff} = 35{,}000$ K if the wind density is low. This is due to the fact that the $n = 1$–2 line of He^+ at 304 Å is optically very thick so that the $n = 2$ level is strongly populated and the ionization to He^{++} is dominated by photoionization from the $n = 2$ level (see Lamers & de Koter 1993). If the expansion of stellar photosphere is taken into account in

TABLE 3

HELIUM RECOMBINATION IN THE WINDS

$< \rho >$ [g cm^{-3}]	$T_{\rm rec}(100\ R)$ [K]	$T_{\rm rec}(10\ R)$ [K]
9.1×10^{-15}	34,500	34,000
3.6×10^{-14}	36,250	35,500
9.1×10^{-14}	39,000	37,500

NOTE.—Helium is He^+ at $r = 10$ R or 100 R if $T_{\rm eff} < T_{\rm rec}(r)$. Helium is He^{++} at $r = 10$ R or 100 R if $T_{\rm eff} \geq T_{\rm rec}(r)$.

TABLE 4

ATOMIC DATA FOR DERIVING $\dot{M}$ FROM RADIO FLUXES

$\frac{He}{H+He}$	X	Y	Z	Ionization			μ_i	γ	$<Z>$	$\frac{\gamma<Z>^2}{\mu_i^2}$
0.10	0.67	0.30	0.03	H^+	He^{++}	Z^{+++}	1.339	1.105	1.149	0.814
				H^+	He^+	Z^{++}	1.339	1.002	1.003	0.562
0.15	0.57	0.40	0.03	H^+	He^{++}	Z^{+++}	1.488	1.154	1.211	0.764
				H^+	He^+	Z^{++}	1.488	1.002	1.004	0.456
0.20	0.485	0.485	0.03	H^+	He^{++}	Z^{+++}	1.645	1.205	1.273	0.722
				H^+	He^+	Z^{++}	1.645	1.003	1.004	0.374

the non–LTE radiative transfer, the He II resonance becomes somewhat desaturated (Gabler et al. 1989).

The values of the constants γ, μ_i, and Z for different helium abundances and for two degrees of ionization are listed in Table 4. We assumed a metal abundance of $Z = 0.03$ and a mean mass per metal ion of $17m_H$ (Allen 1973). The degree of ionization of the metals is related to that of helium. We assumed that the metals, i.e., mainly CNO, are triply ionized if He is doubly ionized and the metals are doubly ionized if He is singly ionized. Anyway, the ionization of the metals has only a very minor effect on the values of the constants. The values of $\dot{M}/v_\infty$, derived from the radio fluxes, are listed in Table 5. Since the result depends on the assumed ionization of helium in the wind we analyzed the data for both assumptions: a wind with He^+ or He^{++}. From the resulting mass-loss rates for both cases we calculated the characteristic density $\langle\rho\rangle$ from equation (6) and the recombination temperature T_{rec} at 10 and 100 R from equations (7) and (8). If $T_{eff} > T_{rec}$, the wind is ionized to He^{++}, whereas the wind is ionized to He^+ if $T_{eff} < T_{rec}$. We then adopted the mass-loss rates derived for the corresponding degree of ionization of He. The mass-loss rates for a wind with He^+ are typically 30% higher than those for He^{++}. This is mainly due to the fact that the factor $\gamma Z^2/\mu^2$ which enters into the mass-loss formula (eq. [4]) is about 30% lower for a wind with He^+ than for He^{++}. In only one case did we find the star to be on the borderline between He^+ and He^{++}, i.e. for the star HD 37043 for which $T_{rec}(10\ R) = 34{,}600$ K and $T_{eff} = 34{,}000$ K. We assumed that helium is mainly He^+ for this star. In Table 5 we indicate for each star the adopted ionization stage of He in the wind between 10 and 100 R.

Wright & Barlow (1975) showed that the net output of free-free radiation emitted by an isothermal wind with constant velocity and constant temperature is equal to the total amount of free-free radiation emitted by the wind layers above some effective radius $r_{eff}(\lambda)$. This effective radius is defined by the condition that the radial optical depth from infinity to r_{eff} is 0.244. Lamers & Waters (1984) showed that this approximation is also valid for nonisothermal and accelerating winds. The effective radius is given by

$$\tau(\lambda) = 0.244$$

$$= 5.3 \times 10^{31}\left(\frac{\dot{M}Z}{v_\infty \mu}\right)^2 \gamma T_e^{-3/2} R^{-3} \lambda^2 g_\nu \int_{r_{eff}/R}^{\infty} w^{-2} x^{-4}\, dx, \quad (9)$$

where R is in $R_\odot$, v_∞ in km s^{-1}, λ is in cm, $x = r/R$ and $w(x) = v(r)/v_\infty$. The values of r_{eff}/R are listed in Table 5. Since the emission of the wind decreases approximately as ρ^{-2}, i.e., as r^{-4}, the bulk of the radio flux is emitted at a distance between r_{eff} and $1.5r_{eff}$. For most of the stars in Table 5 r_{eff} is in the range of 6–50 R at a wavelength of 3.6 cm.

The resulting mass-loss rates are listed in Table 5. The uncertainties given in the last column are based on the uncertainties in S_ν, in v_∞, and in the distance. This latter uncertainty is assumed to be 0.1 dex.

TABLE 5

MASS-LOSS RATES DERIVED FROM RADIO FLUXES

HD	$\frac{\dot{M}}{v_\infty}$ [$\frac{M_\odot yr^{-1}}{km\ s^{-1}}$]					He	r_{eff} [R]	log $\dot{M}$
	1.3 mm	2.0 cm	3.6 cm	6.0 cm	mean		3.6 cm	$M_\odot yr^{-1}$
14947				$< 7.6 \times 10^{-9}$	$< 7.6 \times 10^{-9}$	++		$< -4.76 \pm 0.18$
15570		$< 2.2 \times 10^{-9}$	1.8×10^{-9}	$< 3.6 \times 10^{-9}$	$1.8 \pm 0.4 \times 10^{-9}$	++	13.0	-5.33 ± 0.18
30614				2.5×10^{-9}	$2.5 \pm 0.6 \times 10^{-9}$	+	12.8	-5.41 ± 0.18
36486			5.4×10^{-10}		$5.4 \pm 0.3 \times 10^{-10}$	+	48.5	-5.97 ± 0.15
36861				$< 4.8 \times 10^{-10}$	$< 3.8 \times 10^{-10}$	++		$< -6.04 \pm 0.18$
37043			1.3×10^{-10}		$1.3 \pm 0.3 \times 10^{-10}$	+	25.6	-6.50 ± 0.18
37128	2.5×10^{-9}			2.7×10^{-9}	$2.7 \pm 0.1 \times 10^{-9}$	+	10.5	-5.39 ± 0.16
37742			1.2×10^{-9}	1.3×10^{-9}	$1.2 \pm 0.08 \times 10^{-9}$	+	6.9	-5.60 ± 0.15
57061			3.2×10^{-9}		$3.2 \pm 0.2 \times 10^{-9}$	+	13.5	-5.20 ± 0.15
66811	1.7×10^{-9}	1.3×10^{-9}	1.1×10^{-9}	1.1×10^{-9}	$1.1 \pm 0.1 \times 10^{-9}$	++	12.0	-5.62 ± 0.15
149038				$< 2.5 \times 10^{-9}$	$< 2.5 \times 10^{-9}$	+		$< -5.36 \pm 0.18$
149404			5.0×10^{-9}		$5.0 \pm 0.2 \times 10^{-9}$	+	15.9	-4.91 ± 0.15
149757			2.6×10^{-11}		$2.6 \pm 0.2 \times 10^{-11}$	++	2.3	-7.41 ± 0.16
151804				6.3×10^{-9}	$6.3 \pm 1.2 \times 10^{-9}$	+	18.1	-5.00 ± 0.17
152408	1.8×10^{-8}	1.5×10^{-8}		1.3×10^{-8}	$1.4 \pm 0.1 \times 10^{-8}$	+	37.9	-4.87 ± 0.15
152424			3.1×10^{-9}		$3.1 \pm 0.5 \times 10^{-9}$	+	12.1	-5.26 ± 0.17
210839			1.0×10^{-9}		$1.0 \pm 0.07 \times 10^{-9}$	++	10.7	-5.68 ± 0.15

NOTE.—The uncertainties in col. (6) reflect only the uncertainties in the measured fluxes. The uncertainties in col. (9) reflect the uncertainty in the fluxes as well as in the distances (δ log $D = 0.10$).

4. MASS-LOSS RATES FROM Hα

Hα mass-loss rates for a sample of 149 galactic OB stars have been published by Leitherer (1988; L88). The mass-loss rates given in that paper were based on Hα equivalent widths collected from the literature. The theoretical relation between the observed Hα luminosity and the mass-loss rate had originally been derived by Klein & Castor (1978) for a fixed velocity law. L88 generalized this theoretical relation for arbitrary velocity laws.

In the present paper, we are reevaluating the mass-loss rates published by L88. Several important issues arose since then: (i) Groenewegen & Lamers demonstrated that P Cygni profiles of ultraviolet resonance lines are affected by significant chaotic motions ("turbulence") in the wind. As a consequence, the wind terminal velocities are lower than previously assumed, and therefore $\dot{M}$ is correspondingly lower, too. (ii) The velocity law can accurately be derived by UV line fitting with the SEI method (see above). The quantity $v(r)$ derived from the ultraviolet can be used as an input parameter to derive Hα mass-loss rates. (iii) Gabler et al. (1990) suggested that He II λ6560 may significantly contribute to the observed Hα luminosity. If so, the derived Hα mass-loss rates will be significantly over or underestimated, depending on the absorption or emission of He II λ6560. In view of these new developments we decided to redetermine the relation between the observed Hα equivalent widths and the corresponding $\dot{M}$.

4.1. *The Observed Equivalent Widths of* Hα

Hα equivalent widths in O stars have been measured by Buscombe (1969), Conti (1974), Conti & Frost (1977), Ebbets (1982), Peppel (1984), Rosendhal (1973), and Wilson (1958). We took these results to calculate mean Hα equivalent widths W_{obs} for all program stars except for HD 149404 and HD 149757. No Hα equivalent widths could be found for HD 149404 in the literature. Walborn (1980) published a photographic plate of the red spectral region of this star. Hα of HD 149404 is approximately equally strong as Hα of HD 151408, which has a large Hα equivalent width of 13 Å in emission (see Table 6). The strong Hα emission in HD 149404 is consistent with the high mass-loss rate derived from the radio flux.

HD 149757 is known as a peculiar, variable Oe star. Ebbets (1981) monitored its Hα line over the course of a year and found significant profile variability. W_{obs} varied by a factor of 20 during these observations. Most likely, the profile of Hα and its variations are the consequence of a gas ring close to the stellar surface of HD 149757. It is doubtful that W_{obs} can be related to $\dot{M}$. Therefore we did not include HD 149757 in our sample of stars with observed Hα equivalent widths.

The adopted values of W_{obs} are listed in column (2) of Table 6. The letter "a" denotes absorption and "e" emission. In most cases, W_{obs} does not differ from the values listed by L88. Slight differences are due primarily to inclusion of additional Hα sources as compared to the earlier paper and different weights assigned to Ebbets's measurements, which are now weighted with the number of individual observations. Most equivalent widths are from older photographic measurements obtained by Conti (1974). A quantitative estimate of the reliability of these data is possible via the spectral classification scheme devised by Conti & Alschuler (1971) and Conti & Frost (1977). Their O star classification scheme is based on measured equivalent widths from photographic plates, and any

TABLE 6

MASS-LOSS RATES FROM Hα

HD	W_{obs} (ref) [Å]	W_{phot} [Å]	$W(HeII)$ [Å]	W_{net} [Å]	δW_{net} [Å]	$\log L_{6563}$ [$erg\ s^{-1}$ Å^{-1}]	$\log L(H\alpha)$ [$erg\ s^{-1}$]	v_0 [$km\ s^{-1}$]	$\frac{v_0}{v_\infty}$	I	$c(T_{eff})$	$\log \dot{M}$ [$M_\odot yr^{-1}$]
14947	6.36e (2, 3, 5)	2.6	0.60e	8.36	2.21	33.80	1.14	27	0.012	1.15	−6.53	$-5.32^{+0.18}_{-0.18}$
15558	1.24a (2, 5)	2.6	0.60e	0.76	0.38	33.92	0.22	27	0.008	1.21	−6.57	$-5.61^{+0.19}_{-0.23}$
15570	9.76e (2, 3, 5)	2.5	0.60e	11.7	3.10	34.04	1.53	27	0.010	1.18	−6.57	$-5.02^{+0.18}_{-0.18}$
15629	1.87a (2, 3)	2.8	0.44a	1.37	0.49	33.56	0.11	28	0.010	1.18	−6.61	$-5.77^{+0.18}_{-0.20}$
24912	1.50a (4, 6, 7)	2.6	1.38a	2.48	0.70	33.40	0.21	26	0.011	1.16	−6.46	$-5.89^{+0.18}_{-0.19}$
30614	2.60e (4, 6, 7)	1.8	0.85a	5.25	1.37	34.04	1.18	23	0.015	1.10	−6.29	$-5.47^{+0.18}_{-0.18}$
36486	2.01a (2, 7)	1.7	0.78a	0.47	0.38	33.99	0.08	24	0.012	1.15	−6.35	$-5.92^{+0.21}_{-0.40}$
36861	3.00a (2, 4, 7)	2.5	1.05a	0.55	0.45	33.44	−0.40	25	0.010	1.18	−6.43	$-6.20^{+0.21}_{-0.41}$
37043	2.46a (1, 2, 4, 7)	2.2	0.87a	0.61	0.42	33.72	−0.08	24	0.010	1.18	−6.38	$-5.99^{+0.21}_{-0.31}$
37128	0.44e (4, 6, 7)	1.6	0.36a	2.40	0.67	34.16	0.96	22	0.015	1.10	−6.20	$-5.59^{+0.18}_{-0.18}$
37742	0.42e (2, 4, 7)	1.7	0.74a	2.86	0.78	34.16	1.03	23	0.011	1.16	−6.29	$-5.41^{+0.18}_{-0.18}$
46150	3.31a (2)	2.8	0.44a	−0.07	0.45	33.56	<−0.44	28	0.010	1.18	−6.61	< −5.88
46223	1.91a (2)	2.8	0.44a	1.33	0.49	33.48	0.02	29	0.010	1.18	−6.65	$-5.85^{+0.18}_{-0.20}$
47839	3.08a (4, 7)	2.8	0.83a	0.55	0.45	33.28	−0.56	27	0.012	1.15	−6.52	$-6.30^{+0.21}_{-0.41}$
57061	1.42a (1, 4)	2.2	0.78a	1.56	0.51	34.16	0.77	24	0.012	1.15	−6.38	$-5.54^{+0.18}_{-0.19}$
66811	3.09e (3, 4)	2.7	0.60e	5.19	1.37	33.78	0.91	27	0.012	1.15	−6.57	$-5.45^{+0.18}_{-0.18}$
93129A	8.13e (3)	2.5	0.60e	10.0	2.65	34.16	1.58	30	0.010	1.19	−6.70	$-4.88^{+0.18}_{-0.18}$
149038	0.80a (1, 6)	1.8	0.78a	1.78	0.54	34.04	0.71	23	0.013	1.13	−6.29	$-5.67^{+0.18}_{-0.19}$
151804	13.2e (2)	2.2	0.78a	16.2	4.27	34.28	1.91	24	0.015	1.10	−6.38	$-5.00^{+0.18}_{-0.18}$
152408	34.7e (2)	2.2	0.78a	37.7	10.1	34.16	2.15	24	0.025	0.97	−6.38	$-5.07^{+0.18}_{-0.18}$
152424	0.64e (2)	1.7	0.78a	3.12	0.84	34.20	1.11	23	0.013	1.13	−6.29	$-5.42^{+0.18}_{-0.18}$
164794	2.11a (2, 4)	2.8	0.44a	1.13	0.46	33.80	0.27	29	0.010	1.18	−6.65	$-5.62^{+0.19}_{-0.20}$
188001	3.16e (2, 4)	2.4	0.78a	6.34	1.64	34.00	1.22	24	0.013	1.13	−6.38	$-5.38^{+0.18}_{-0.18}$
190429A	7.94e (3)	2.5	0.60e	9.84	2.60	33.96	1.37	27	0.012	1.15	−6.57	$-5.16^{+0.18}_{-0.18}$
190864	1.83a (2, 5)	2.6	0.44a	1.21	0.46	33.60	0.10	26	0.011	1.16	−6.51	$-5.88^{+0.18}_{-0.20}$
210839	1.78e (2, 4, 7)	2.4	0.44a	4.62	1.21	33.88	0.96	26	0.012	1.15	−6.48	$-5.46^{+0.18}_{-0.18}$

REFERENCES.—(1) Buscombe 1969; (2) Conti 1974; (3) Conti & Frost 1977; (4) Ebbets 1982; (5) Peppel 1984; (6) Rosendhal 1973; (7) Wilson 1958.

significant errors would result in a spectral type different from other classification schemes. For instance, a difference in the logarithmic ratio of W_{4471} and W_{4541} by more than ~ 0.1 dex modifies the spectral types by more than half a subtype between types O5.5 and O9. In general, there is very good agreement between Conti's temperature classification and one of Walborn & Fitzpatrick (1990), which is based on CCD data. This indicates that older equivalent widths based on photographic spectrograms are reliable to within 10%. In any case, as we will show below, other uncertainties (like wind variability) produce larger error bars so that the older equivalent-width determinations are sufficient for our purpose.

In order to derive the net wind emission from the observed equivalent width of Hα, the underlying photospheric Hα absorption must be accounted for. Scuderi et al. (1992) demonstrated that the optical depth at the line center of Hα formed in the wind is comparable to or smaller than unity in O stars. In this case, the net wind emission follows from simple arithmetic subtraction of the assumed photospheric absorption. Gabler et al. (1989, 1990) published self-consistent models for expanding stellar atmospheres without the artificial separation between photospheric absorption and wind emission. Their results support the model calculations of Scuderi et al. in the range $-6.0 < \log \dot{M} < -5.0$, which is the most relevant for this study.

Additional support for this procedure comes from the observed Hα line profiles (see Conti & Frost 1977). Those stars displaying the strongest emission (like, e.g., HD 151804), and therefore having the largest optical depth, are characterized by emission profiles more or less symmetrical with respect to the rest wavelength of the star. This suggests no significant wind absorption on the blue side of the profile. Only in a few cases—HD 66811 being the most prominent example—P Cygni-like profiles with a blueshifted absorption component are present. The equivalent widths of the absorption components, however, are small in comparison with the emission components. We did not correct the net wind emission for the presence of the absorption component of the P Cygni profile—e.g., by adopting twice the equivalent width of the emission redward of the rest wavelength. First, because most authors did not discriminate between the absorption and emission parts of Hα (if present), and only integrated equivalent widths of Hα were published. More importantly, since $\dot{M}$ scales with the square root of the wind luminosity in Hα, such a correction is of rather minor importance. The derived mass-loss rates are *underestimated* by less than 0.05 dex without such a correction. Therefore no such correction has been applied. We used the equivalent widths following from Auer & Mihalas's (1972) non–LTE line profiles to assign photospheric Hα absorptions $W_{\rm phot}$ to each program star (col. [3] of Table 6). The photospheric Hα absorption strengths of most stars are very similar due to the weak temperature dependence of $W_{\rm phot}$ above $T_{\rm eff} \approx$ 30,000 K. The sensitivity $W_{\rm phot}$ to changes in $\log g$ is quite moderate. This is relevant for the question of the uncertain stellar masses, which of course would affect $\log g$. An uncertainty of 0.2 dex in M (and therefore in g) leads to an uncertainty of about 0.2 Å for $W_{\rm phot}$ of O stars. The corresponding error in the net wind emission is completely negligible for all but the very lowest mass-loss rates. We also compared the values for $W_{\rm phot}$ published by Auer & Mihalas to those of Mihalas (1972) which were calculated under the assumption of a different broadening theory. No significant difference was found.

4.2. *The Effect of the* He II λ6560 *Line*

Hα overlaps in wavelength with the He II $n = 4 \rightarrow 6$ Pickering transition at 6560 Å. Gabler et al. (1989, 1990) presented theoretical models for hydrogen and helium lines in an O star having parameters similar to HD 66811. They found He II λ6560 in emission with an equivalent width comparable to the one of the Hα emission. Therefore they concluded that mass-loss rates derived from the Hα strength without correcting for the He II λ6560 blend will be overestimated by typically 0.2 dex. Since He II λ6560 obviously is not accessible to direct measurements, there is no straightforward observational test to prove or reject such a theoretical prediction. However, Gabler et al.'s models also predict the strengths of those Pickering lines not coinciding with Balmer lines, in particular the strength of the $n = 4 \rightarrow 5$ transition at 10124 Å. The He II λ10124 has been observed in a sample of O stars by Mihalas & Lockwood (1972). We use these data to investigate the importance of He II Pickering line emission with respect to Hα.

Mihalas & Lockwood (1972) measured He II λ10124 in 12 hot stars, including ζ Pup. The line is found to be in absorption in all stars except ζ Pup, where an equivalent width of 2.3 Å in emission is observed. In contrast, Gabler et al. (1989) predict a much stronger emission of about 10 Å for this line. They assumed $\dot{M} = 6 \times 10^{-6}\ M_\odot\ {\rm yr}^{-1}$, which is higher than found in the present study. Their model with $\dot{M} = 3 \times 10^{-6}\ M_\odot\ {\rm yr}^{-1}$ predicts an emission-line strength of about 4 Å for He II λ10124, which would be closer to the observations. However, in this case the Hα emission would be too weak to reproduce the observations, which require a mass-loss rate of $\dot{M} = 6.3 \times 10^{-6}\ M_\odot\ {\rm yr}^{-1}$ (Gabler et al. 1990). Gabler et al.'s models fail to reproduce Hα and He II λ10124 simultaneously. Since the relative strengths of the $n = 4 \rightarrow 5$ and the $n = 4 \rightarrow 6$ transitions are primarily controlled by atomic physics, we expect that Gabler et al.'s models overestimate the emission strength of He II λ6560 in a similar way.

In order to account for the blending effect of He II λ6560 on Hα, we chose a purely empirical approach. We assumed that the strength of the $n = 4 \rightarrow 6$ transition can be approximated by the arithmetic mean of the strengths of the $n = 4 \rightarrow 5$ and $n = 4 \rightarrow 7$ (5411 Å) transitions. This is a rather crude method but at least for stars with He II λ10124 clearly in absorption, it is a reasonable first-order estimate. Fortunately, He II λ10124 is—or can be expected to be—in absorption for all but five program stars (cf. Table 6). Conversely, if He II λ10124 is not in absorption, Hα itself is strongly in emission since this corresponds to the case of the highest mass-loss rates, and the contribution of He II λ6560 to Hα becomes negligible.

Test calculations for a late and an early O star (W. Schmutz, private communication) suggest that it is a reasonable first-order approximation to add the equivalent widths of Hα and He II λ6560 individually in order to calculate the combined equivalent width of Hα + He II λ6560. Any error which is introduced by this method will mostly affect stars with low mass-loss rates since for those stars the correction of Hα for He II contamination is largest. On the other hand, the correction of Hα for the presence of He II λ6560 is negligible for stars with intermediate and high mass-loss rates (cf. Table 6).

The equivalent widths of He II λ10124 have been taken from the observations by Mihalas & Lockwood (1972) and those of He II λ5411 from Conti (1974), Conti & Frost (1977), and Wilson (1958). Empirical 6560 Å equivalent widths for all 12 stars of Mihalas & Lockwood's sample were computed. Nine of these stars are included in our list of program stars (HD

24912, HD 30614, HD 36861, HD 37043, HD 37128, HD 37742, HD 47839, HD 66811, HD 210839), and their values of W(He II) are given directly in column (4) of Table 6. We attempted to establish a relation between W(He II) and stellar parameters in order to predict W(He II) for those program stars which have not been observed by Mihalas & Lockwood. No tight relationship could be derived. The range of W(He II) extends from slight emission (-0.6 Å) in the earliest O supergiants to moderate absorption (0.8 Å) for late O stars. We adopted the following rules for those stars not observed by Mihalas & Lockwood: late O stars of all luminosity classes—0.78 Å in absorption; supergiants earlier than O6—0.60 Å in emission, i.e. the value derived for ζ Pup; early-O dwarfs and mid-O supergiants—0.44 Å in absorption as derived for in HD 210839. The results can be found in column (4) of Table 6. Note that W(He II) is fairly uniform over the entire stellar sample, suggesting only a weak temperature and luminosity dependence.

4.3. *The Mass-Loss Rates Derived from the Observed* Hα *Emission*

Column (5) of Table 6 gives the net equivalent width of the wind emission ($W_{\rm net}$). $W_{\rm net}$ follows from $W_{\rm obs}$ after correction for photospheric Hα absorption and He II absorption or emission:

$$W_{\rm net} = {\rm sign}_1\ W_{\rm obs} + W_{\rm phot} - {\rm sign}_2\ W({\rm He\ II})\ . \qquad (10)$$

${\rm sign}_1 = +1$ or -1 for $W_{\rm obs}$ in emission or absorption, respectively; ${\rm sign}_2 = +1$ or -1 for W(He II) in emission or absorption, respectively. Column (6) of the table lists the errors of $\delta W_{\rm net}$. Three effects have been assumed to affect $W_{\rm net}$: (i) the observed equivalent widths are influenced by systematic errors due to the choice of the continuum, telluric absorption lines which are abundant in this wavelength region, and due to statistical noise. A 10% error has been assigned to all those effects; (ii) O star winds are variable (see Ebbets 1982). Conti & Niemela (1976) reported changes in the Hα equivalent width of ζ Pup of about 25%. We suspect that such variations may be present in all O star winds and assume an uncertainty of 25% for $W_{\rm net}$ due to wind variability; (iii) correction for photospheric Hα and He II emission/absorption introduces a further uncertainty. We estimate that $W_{\rm net}$ may be affected by up to 0.3 Å due to this effect. Combining all three error sources we derived $\delta W_{\rm net}$ for all program stars. $W_{\rm net}$ is larger than 0 in all but one case due to emission from stellar winds. The main-sequence star HD 46150 has $W_{\rm net} = -0.07 \pm 0.45$ Å, consistent with very little wind emission.

The stellar luminosity per unit wavelength of the continuum at 6563 Å, L_{6563}, can be derived from M_V, together with the absolute visual magnitude of the Sun (Allen 1973), and the gradient of the continuum between the V passband and Hα:

$$\log\,(L_{6563}) = -0.4M_V + 31.63 + \log\frac{F({\rm H}\alpha)}{F(V)}\ . \qquad (11)$$

Log $[F({\rm H}\alpha)]/[F(V)]$ has been taken from the LTE model-atmosphere predictions of Kurucz (1979). We found log $[F({\rm H}\alpha)]/[F(V)] = -0.27$ for all program stars. The results for log (L_{6563}) are in column (7) of Table 6. Subsequently, the wind luminosity in Hα has been obtained from $W_{\rm net}$ and the stellar luminosity at 6563 Å in solar units (col. 8):

$$\log L({\rm H}\alpha) = \log\,(L_{6563}) + \log\,(W_{\rm net}) - \log L_\odot\ . \qquad (12)$$

L(Hα) is the luminosity of the wind in Hα due to optically thin recombination radiation of hydrogen originating in the wind. L(Hα) can be related to the stellar mass-loss rate assuming an isothermal, isotropic stationary outflow from the star (L88):

$$\log \dot{M} = 0.5\log L({\rm H}\alpha) + \log v_\infty + 0.5\log R - 0.5I - 0.5c(T_{\rm eff}) - 12.563\ , \qquad (13)$$

where $\dot{M}$ in $M_\odot\ {\rm yr}^{-1}$; L(Hα) in $L_\odot$; v_∞ in km s^{-1}; $R = R_\odot$. I is essentially the distance-integrated velocity law which enters into the expression of the emission measure and has been defined in L88. I depends on the ratio of the initial and terminal velocity of the wind and on the exponent β of the velocity law. We adopted the value of the local sound speed at $T_e = 0.9T_{\rm eff}$ for the initial velocity v_0 (see col. [9] of Table 6). The quantity v_0/v_∞ is given in column (10). The quantity v_∞ (as well as all other stellar parameters entering in eq. [13]) are taken from Table 1. The values derived for I (col. [11]) are based on $\beta = 0.70$ (see § 2). Variations in v_0/v_∞ have only a very minor influence on the derived mass-loss rates: e.g., increasing the value from 0.01 to 0.02 increases $\dot{M}$ by 0.08 dex if $\beta = 0.70$ (cf. Fig. 2 of L88).

The quantity $c(T_{\rm eff})$ incorporates the electron-temperature-sensitive factors of the non–LTE Saha equation and has been computed for $T_e = 0.9T_{\rm eff}$ (col. [12]). Figure 1 of L88 shows $c(T_{\rm eff})$ versus $T_{\rm eff}$ for this case. The quanitity $c(T_{\rm eff})$ is only a weak function of T_e. For instance, if $T_e = 0.8T_{\rm eff}$ had been adopted instead of $0.9T_{\rm eff}$, the corresponding mass-loss rates would have been smaller by typically 0.05 dex.

Column (13) tabulates the mass-loss rates derived via equation (13) for all program stars. The values are between $10^{-4.9}$ $M_\odot\ {\rm yr}^{-1}$ and slightly below $10^{-6}\ M_\odot\ {\rm yr}^{-1}$. The errors given have been calculated using the errors derived for $W_{\rm net}$ and the uncertainties associated with the stellar parameters listed in Table 1. We assumed errors of 0.2 and 0.1 for I and $c(T_{\rm eff})$, respectively. Since the Hα wind emission becomes increasingly small as compared to the photospheric absorption, the mass-loss rates are not very well constrained below $10^{-6}\ M_\odot\ {\rm yr}^{-1}$.

There is essentially no change in the overall mass-loss rates of all stars in comparison with the values derived by L88. Excluding stars with upper limits we find for the mean difference log $\dot{M}$ (this paper) $-$ log $\dot{M}$(L88) $= -0.05 \pm 0.18$. This difference is the result of a combination of several factors. Above all, the terminal velocities adopted here are somewhat smaller than in L88 leading to slight decrease in $\dot{M}$. In addition, there are slight changes in the adopted stellar parameters which affect $\dot{M}$ in some cases.

A further modification is introduced by accounting for He II λ6560. The overall effect is that the derived $\dot{M}$ is generally slightly *higher*. He II λ6560 is slightly in emission for the earliest types and for the most luminous stars. In those stars, however, Hα is a very strong emission line and the He II contribution is insignificant. In contrast, He II λ6560 is a moderately strong photospheric absorption line in less luminous and in cooler stars where Hα is *not* strongly in emission. In this case, the He II correction will increase the derived $\dot{M}$ although the effect is hardly significant (an increase in 0.15 dex in the worst case). Kudritzki et al. (1991) decreased all mass-loss rates derived by L88 by 0.2 dex to account for the He II blend. Our new empirical analysis presented here suggests that Hα mass-loss rates are generally *not* overestimated if He II λ6560 is not taken into account.

The most important difference between the mass-loss rates derived here and those derived by L88 is with respect to the

adopted velocity law. Here we made use of the result of Groenewegen & Lamers (1989) and used a uniform $v(r)$ with $\beta = 0.70$ for all O stars. In contrast, L88 derived the velocity law by comparing stars having ultraviolet and Hα mass-loss rates. Subsequently, the derived $v(r)$ was found to be dependent on $T_{\rm eff}$, and an appropriate $v(r)$ was applied for each spectral type to derive $\dot{M}$. Despite the $T_{\rm eff}$ dependence, the average $v(r)$ for O stars turned out to have $\beta = 0.7$ in that study. This explains why the average mass-loss rates have hardly changed between the earlier paper and this study. However, the new mass-loss rates are lower by about 0.2 dex for the earliest spectral types, and they are higher for the latest types by 0.2 dex. This is due to a steeper (shallower) velocity law adopted by L88 for the earliest (latest) O stars as compared to the new study.

5. COMPARISON BETWEEN THE MASS-LOSS RATES FROM RADIO FLUXES AND Hα

Our approach of deriving $\dot{M}$ from the Hα luminosity differs from L88's method in an important aspect. L88 scaled the Hα mass-loss rates to match the observed ultraviolet rates, which in turn had been calibrated before by radio mass-loss rates. Ultimately, the mass-loss rates in L88 were not independent from radio mass-loss rates. The approach used in the present study is different. Ultraviolet data are taken only to provide *velocity* information, i.e., β and v_∞ but not $\dot{M}$. As shown by Groenewegen & Lamers (1991), the uncertain ionization fractions of C^{3+}, N^{4+}, and Si^{3+} in O star winds preclude reliable determinations of mass-loss rates. On the other hand, the velocity law can be readily derived by a line-fitting technique.

Since the radio rates of § 3 and the Hα rates of § 4 have been derived independently, a comparison of $\dot{M}$ from the two methods provides an important test of the reliability of our results. In Figure 2 we compare $\dot{M}$ derived from the radio and from Hα. The figure includes all stars of Table 5 with radio mass-loss rates (as well as three stars with upper limits), except HD 149404 and HD 149757 for which no Hα data were available. The agreement between the radio and Hα rates is good.

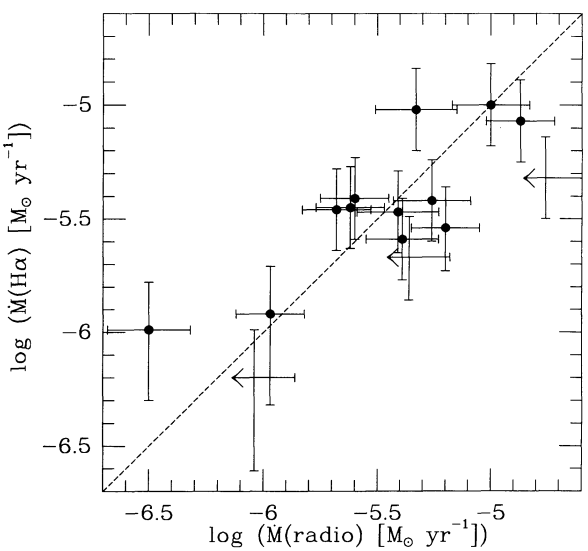

FIG. 2.—Comparison between $\dot{M}$ derived from radio data and from Hα. ← denotes stars with upper limits for the radio fluxes.

We find a difference of $\log \dot{M}(\mathrm{H}\alpha) - \log \dot{M}(\mathrm{radio}) = +0.03 \pm 0.23$. This suggests that the radio and Hα methods are equally reliable once the velocity law of the wind has been derived independently. The observational errors of the two methods are comparable if $\dot{M} > 10^{-5.5}\ M_\odot\ \mathrm{yr}^{-1}$. If this is the case, the errors are dominated by uncertainties in the adopted stellar parameters and not by errors of the measurement itself. Radio rates are predominantly affected by the distance uncertainty. The errors in the Hα rates are mostly due to the error in the stellar radius (i.e., distance and bolometric correction) and in the adopted velocity law. Note that an error of 0.1 in β introduces an error of ~ 0.2 in I, and therefore an error of 0.1 in $\log \dot{M}$ (cf. eq. [3]). If mass-loss rates are less than approximately $10^{-5.5}\ M_\odot\ \mathrm{yr}^{-1}$, Hα mass-loss rates become increasingly uncertain due to the subtraction of the underlying photospheric absorption profile. This is obvious from the large negative error bars in Figure 2. Radio data of O stars with such low mass-loss rates are relatively sparse due to the low flux densities at cm wavelengths.

We conclude from Figure 2 that radio and Hα data lead to consistent values of $\dot{M}$ over a range of more than an order of magnitude. Since both methods are independent, this suggests that there are no significant systematic errors present in the two data sets. Only if v_∞ were significantly in error, radio and Hα would be affected by a systematic error acting in the same direction. Our result disagrees with the conclusion of Abbott, Bieging, & Churchwell (1981) who found no correlation between the radio and Hα mass-loss rates of a sample of luminous OB stars. The reason for the discrepancy is the inclusion of several stars in their sample which were subsequently recognized to be nonthermal radio emitters (9 Sgr, Cyg OB2 no. 8A, Cyg OB2 no. 9) and an uncertain radio detection of Cyg OB2 no. 7. Excluding those stars in their Figure 5, Abbott et al.'s sample exhibits the same good correlation between $\dot{M}$(radio) and $\dot{M}(\mathrm{H}\alpha)$ as ours.

Our result differs from Drew's (1990) conclusion that Hα mass-loss rates are higher than radio mass-loss rates by a factor of 2 if $\beta = 0.7$ is adopted. Drew calculated wind models for a grid of stellar parameters using the relation

$$\dot{M} = 7.4 \times 10^{-8} \left(\frac{L}{10^5}\right)^{1.72}, \qquad (14)$$

with $\dot{M}$ in $M_\odot\ \mathrm{yr}^{-1}$ and L in $10^5\ L_\odot$. Using equation (14), an Hα wind luminosity was calculated for the entire model grid, and the Hα luminosity is parameterized in terms of stellar parameters. Drew compared the resulting Hα mass-loss rates to radio mass-loss rates of seven stars assuming a $\beta = 0.7$ velocity law. It turns out that the Hα rates are, on average, higher by a factor of 2 than the radio rates. If the observed radio mass-loss rates are adopted, the theoretical Hα luminosities agree with the observed Hα data only if a relatively flat velocity law with $\beta = 1.5$ is assumed.

What is the reason for the difference? Inspection of Drew's Table 4 shows that the radio mass-loss rates used for the comparison with her Hα rates are inconsistent with equation (14). Excluding Cyg OB2 No. 9, which has extremely uncertain stellar parameters, we find that the radio mass-loss rates given in column (4) of Drew's Table 4 are higher by 0.32 dex than predicted by equation (14). Since the scaling relation for $\log L(\mathrm{H}\alpha)$ in Drew's paper was derived from a relation between $\dot{M}$, v_∞, and R, we would expect a different relation if the mass-loss rates for given stellar parameters were higher. Only detailed calculations could support or reject this suggestion.

We also note that the temperature structure of the wind adopted by Drew differs from the one adopted here, in the sense that Drew's temperature is lower in the Hα emitting region. This may contribute to the enhanced wind absorption in Hα found by Drew. Such an effect could well contribute to the differences in the two methods. Clearly detailed Hα profile analyses are required to constrain the wind temperatures and velocity law to a degree which allows one to settle this issue.

Both the radio and the Hα emission can be affected by inhomogeneities in the winds. If significant clumping were present in the winds, the mass-loss rates which are derived under the assumption of a uniform density via the equation of continuity will be overestimated. The effect of clumping on the mass-loss rates derived from the radio-flux was described by Abbott et al. (1981) for isothermal clumping and by Lamers & Waters (1984b) for nonisothermal clumping. Abbott et al. showed that the mass-loss rate derived from radio data in an isothermal clumpy wind is proportional to

$$\dot{M} \propto \frac{f + x(1-f)}{[f + x^2(1-f)]^{1/2}}, \tag{15}$$

where f is the volume-filling factor of the dense clumps and x is the density contrast between the clumps and low-density gas and the high-density clumps. Owocki (1992, and references therein) has shown that shocks in the winds of O stars could produce significant clumping with very high density contrasts of $x \approx 10^{-2}$ to 10^{-3}. In that case $\dot{M} \propto f^{-1/2}$. The most extreme model of Owocki, with $\delta\rho/\rho = 0.25$ at the base of the wind, has a filling factor $f \approx 10$ already at $r = 1.1\ R$. For less extreme models the shocks develop at larger heights of $r \approx 2\ R$ and the filling factors are less severe.

Since the clumping in the wind cannot be predicted accurately we may use the observational evidence to estimate its effect on the mass-loss determinations. We think that clumping does not seriously affect our estimates of the mass-loss rates, for the following reasons.

1. First, we note that the Hα variability observed in some (or even all) O stars cannot be used as an argument in favor of clumping. Ebbets (1982) investigated the time scales associated with significant Hα variability. No significant Hα variability with time scales comparable to the flow time scales (~hours) was found. In contrast, Hα varied on time scales of days to months. This may suggest a connection between the Hα and mass-loss variability with photospheric and/or structural variations, which are characterized by the dynamical time scale, rather than by inhomogeneities of the outflow, which are associated with the flow time scale.

2. For the four stars (HD 37128, HD 37742, HD 66881, and HD 152408) for which we have reliable radio fluxes at different wavelengths, i.e., generated at different levels in the wind, the mass-loss rates derived from the fluxes at short wavelengths are very similar to those at 6 cm although the effective radii (§ 3, eq. [9]) at 2 cm and 1.3 mm are smaller than at 6 cm by a factor of 0.5 and 0.08, respectively. This suggests that clumping does not seriously affect the mass-loss estimates from the radio data. Only the two stars HD 66811 and HD 152408 show a slight and systematic increase in mass loss towards shorter wavelengths at $\lambda \leq 2$ cm. For those stars we have adopted the mass-loss rates derived from the 3.6 or 6 cm radio fluxes.

3. Since both free-free and bound-bound emission scale with ρ^2, radio and Hα mass-loss rates would be affected in the same way if the clumping factors were the same in the radio- and Hα-emitting regions. However, Hα originates at a distance of $r \lesssim 2\ R$ whereas the radio flux is observed at distances $r > 10\ R$ (cf. Table 5). Unless the clumping happens to be exactly the same in these two different wind regions, we would expect the Hα flux to be affected in a different way than the radio flux by inhomogeneities in the wind. The agreement between the radio and Hα mass-loss rates suggests that clumping does not influence the derived $\dot{M}$.

6. COMPARISON BETWEEN THE OBSERVED AND PREDICTED VALUES OF $\dot{M}$ AND v_∞

6.1. *Predictions of $\dot{M}$ and v_∞*

The mass-loss rates and the terminal velocities derived from the observations will be compared with the values predicted by the radiation-driven wind models. For this purpose we use the analytic solutions for the wind models given by Kudritzki et al. (1989). These authors have shown that the elaborate numerical solutions of the radiative and dynamical equations which describe the process in winds driven by very large numbers of line transitions can also be obtained by a simple algorithm. In this algorithm several complicated factors that enter the full solutions of the equations are approximated by simple fitting functions. This results in a very elegant set of mathematical expressions that reproduce the observed mass-loss rate and the terminal velocity of an O star to an accuracy of about 10% in $\dot{M}$ and 5% in v_∞.

The radiation pressure by the large number of lines is expressed in terms of the force-multiplier parameters, k, α, and δ, introduced by Castor, Abbott, & Klein (1975) and Abbott (1982). The radiation force can be written as

$$f_{\rm rad}(\text{lines}) = f_{\rm rad}(\text{electrons}) M(t), \tag{16}$$

where $M(t)$ is the force multiplier parameter which depends on the optical depth t, with

$$M(t) = k\left[\frac{\sigma_e \rho v_{\rm th}}{dv/dr}\right]^{\alpha}\left[\frac{n_e}{W(r)}\right]^{\delta} CF. \tag{17}$$

In this expression $v_{\rm th}$ is the thermal velocity of the protons, $\sigma_e \rho$ is the Thompson scattering coefficient per unit mass, n_e is the electron density, $W(r)$ is the geometrical dilution factor and CF is a geometrical factor that takes the finite size of the stellar photosphere into account. Basically, k depends on the number of lines that produce the radiation pressure, α describes the strength or saturation of the driving lines with $\alpha = 1$ if all the lines were saturated and $\alpha = 0$ if none of the driving lines were saturated, and δ describes the change of the ionization through the wind of the ions that produce the radiation pressure.

The values of the force parameters have been calculated by Pauldrach et al. (1990) by solving the full multilevel non–LTE population rates of 133 ionization stages of 26 elements. The radiation pressure due to more than 10^5 line transitions were calculated and the result was expressed in terms of k, α, and δ. Pauldrach et al. (1990) published the values of the force multiplier parameters for a grid of models of massive stars in the range of $T_{\rm eff}$ from 30,000 to 50,000 K and effective gravities of $\log g_{\rm eff}$ between 2.42 and 3.82. These values of k, α, and δ are plotted versus $T_{\rm eff}$ in Figure 3. We eliminated the values of the force multiplier parameters of the models which are close to the Eddington limit, i.e., those with $\Gamma > 0.8$ since none of our program stars reaches such a high value of Γ. Figure 3 shows that the values of k, which largely determine the mass-loss

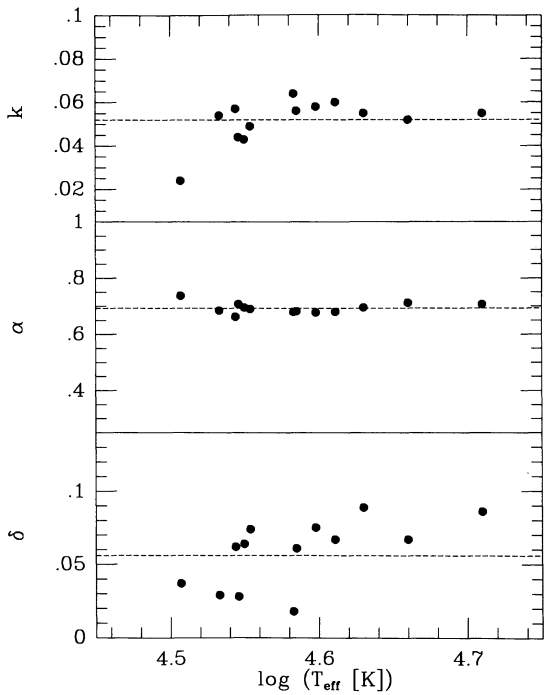

FIG. 3.—Force-multiplier parameters k, α, and δ vs. $T_{\rm eff}$. The individual symbols are from Pauldrach et al. (1990). The dashed lines indicate the mean relations used in the present paper.

rates, are in the range of 0.043–0.060, with a mean value of $k = 0.052 \pm 0.010$. We adopt this mean value. The coolest model of $T_{\rm eff} = 30{,}000$ K has a lower value than adopted. This implies that our predicted mass-loss rates for the stars with $T_{\rm eff} < 33{,}000$ K might be overestimated by about a factor of 2.

The values of α are in the range of 0.662–0.737 with a mean value of $\alpha = 0.693 \pm 0.02$. The values of δ show a considerable variation between 0.018 and 0.086 with a mean value of $\delta = 0.056 \pm 0.023$. Fortunately, this uncertainty in δ has little effect on the predicted values of $\dot{M}$ and v_∞, as we will show below. We adopt the mean values of k, α, and δ. These values are identical to the ones used by Kudritzki et al. (1992).

We should note here that the values of k, α, and δ computed by Pauldrach et al. (1990) are based on the solar abundances of Holweger (1979). These abundances are approximately the same as the more recent compilation by Grevesse & Anders (1989). These abundances are about a factor of 2 higher than those of the Orion Nebula (Peimbert, Torres-Peimbert, & Ruiz 1992). Cunha & Lambert (1992) determined oxygen abundances for a sample of 18 B stars in the Orion OB1 association. The stellar oxygen abundances closely match the oxygen abundance of the Orion Nebula itself. This is expected as the composition of the nebula should reflect the interstellar chemistry at the epoch those stars were formed, and no significant chemical evolution has occurred since then. (This argument is valid only if depletion by dust grains can be neglected.) Abundance determinations from nebular and stellar analyses are entirely independent, and their close agreement gives confidence in the derived oxygen (and other heavy-element) abundances. Five program stars of our sample (HD 36486, HD 36861, HD 37043, HD 37128, HD 37742) are also members of Orion OB1 (Humphreys 1978). Most probably, these stars have oxygen abundances similar to those studied by Cunha & Lambert (1992). We may speculate that *all* our program stars could have oxygen abundances which are closer to those of H II regions in the solar vicinity than to those of the Sun. The radiative acceleration in stellar winds is predominantly dependent on the strength of lines due to the CNO and possibly the Fe group (Abbott 1982). If these lines follow the same trend as the oxygen lines, the values of k and α should have been reduced and the predicted mass-loss rates would be lower since $\dot{M} \propto k^{1/\alpha}$ (Kudritzki et al. 1987).

In order to test the accuracy of our predicted values of $\dot{M}$ and v_∞, we calculated these values for the same grid of stars for which Pauldrach et al. (1990) calculated the detailed wind models by solving the radiative and dynamical equations. The result is shown in Figure 4. The predictions agree with the exact calculations within about 0.2 dex in $\dot{M}$ and within about 400 km s^{-1} in v_∞. The most discrepant mass-loss rate and

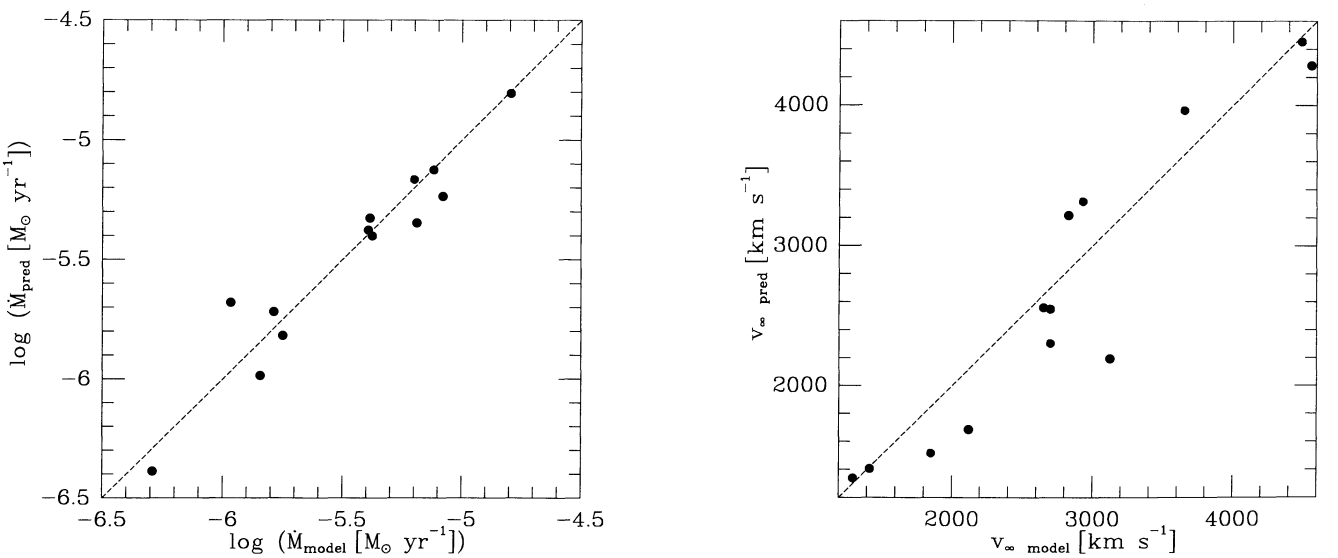

FIG. 4.—Comparison between $\dot{M}$ (*left*) and v_∞ (*right*) predicted by the scaling relations of Kudritzki et al. (1989) and those computed by Pauldrach et al. (1990). "pred" denotes the results of the scaling relations and "model" stands for the exact wind solutions.

velocity shown in Figure 4 is for model C4 of Pauldrach et al. which has $T_{\rm eff} = 32{,}170$ K. This is due to the fact that the values of k and α are respectively lower and higher than our adopted mean values (see Fig. 3). We conclude that our predictions of $\dot{M}$ and v_∞ are accurate within about 0.2 dex in $\dot{M}$ and about 400 km s^{-1} in v_∞ except for stars of $T_{\rm eff} < 33{,}000$ K, where our predictions may overestimate $\dot{M}$ and underestimate v_∞.

6.2. *The Accuracy of the Predicted Values of $\dot{M}$ and v_∞*

We have derived the dependence of $\dot{M}$ and v_∞ on k, α, and δ by calculating the mass-loss rates and v_∞ of nine program stars for different values of the force multiplier parameters. They are listed in Table 9 and discussed in § 7. For the moment we are interested in the mean values of the gradients:

$$\frac{d(\log \dot{M})}{d(k)} \approx +1.0\,, \quad \frac{d(\log \dot{M})}{d(\alpha)} \approx +5.8\,, \quad \frac{d(\log \dot{M})}{d(\delta)} \approx +0.1\,, \tag{18}$$

$$\frac{d(\log v_\infty)}{d(k)} \approx \pm 0.0\,, \quad \frac{d(\log v_\infty)}{d(\alpha)} \approx +1.7\,, \quad \frac{d(\log v_\infty)}{d(\delta)} \approx -0.9\,. \tag{19}$$

Using these derivatives we can estimate the uncertainty in the predicted values of $\dot{M}$ and v_∞ due to the uncertainties in k, α, and δ quoted above. The uncertainties are about 0.12 dex in $\dot{M}$ and 0.04 dex in v_∞.

6.3. *Comparison between Predicted and Observed Values of $\dot{M}$ and v_∞ of the Program Stars*

Using the analytic expressions from Kudritzki et al. (1989) and the values of k, α, and δ described above, we predicted the mass-loss rates and terminal velocities of all our program stars. The results are given in Table 7. This table shows the existence of systematic differences between the observed and predicted values of v_∞ and $\dot{M}$. The values of $v_{\infty\,\rm pred}$ are systematically larger than the observed values by about a factor of 1.4. This same discrepancy is found for all three luminosity classes. The values of $\dot{M}_{\rm pred}$ are systematically smaller than the observed values with a mean ratio of -0.41 ± 0.05 dex for stars of luminosity class I stars, -0.20 ± 0.13 dex for classes II and III, and -0.12 ± 0.14 dex for class V stars.

In order to investigate the cause of the systematic differences between the predictions and the observations, we plotted the

TABLE 7

COMPARISON BETWEEN OBSERVED AND PREDICTED v_∞ AND $\dot{M}$

HD	Type	T_{eff} [10^3 K]	$v_{\infty\ obs}$ [km s^{-1}]	$v_{\infty\ pred}$ [km s^{-1}]	$\frac{v_{\infty\ pred}}{v_{\infty\ obs}}$	log $\dot{M}_{obs}$ [$M_\odot yr^{-1}$]	Method	log $\dot{M}_{pred}$ [$M_\odot yr^{-1}$]	log $\frac{\dot{M}_{pred}}{\dot{M}_{obs}}$
				Class I and f					
93129A	O3 I	50.5	3050 ± 60	4430	1.452	$-4.88^{+0.18}_{-0.18}$	H	−5.30	−0.42
15570	O4 I	42.4	2600	3470	1.335	$-5.33^{+0.18}_{-0.18}$	R	−5.52	−0.19
66811	O4 I	42.4	2200 ± 60	3740	1.700	$-5.62^{+0.15}_{-0.15}$	R	−5.86	−0.24
190429A	O4 I	42.4	2300 ± 70	3580	1.556	$-5.16^{+0.18}_{-0.18}$	H	−5.63	−0.47
14947	O5 f	40.3	2300 ± 70	3370	1.465	$-5.32^{+0.18}_{-0.18}$	H	−5.87	−0.55
210839	O6 I	38.2	2100 ± 60	3170	1.509	$-5.68^{+0.15}_{-0.15}$	R	−5.86	−0.18
151804	O8 I	34.0	1600 ± 70	2330	1.456	$-5.00^{+0.17}_{-0.17}$	R	−5.43	−0.43
152408	O8 I	34.0	960 :	2510		$-4.87^{+0.15}_{-0.15}$	R	−5.61	−0.74
188001	O8 I	34.0	1800 ± 70	2660	1.478	$-5.38^{+0.18}_{-0.18}$	H	−5.84	−0.46
149404	O9 I	32.0	2450	2240	0.914	$-4.91^{+0.15}_{-0.15}$	R	−5.55	−0.64
30614	O9.5 I	30.9	1550 ± 60	2350	1.516	$-5.41^{+0.18}_{-0.18}$	R	−5.92	−0.51
37742	O9.5 I	30.9	2100 ± 150	2210	1.052	$-5.60^{+0.15}_{-0.15}$	R	−5.74	−0.14
149038	O9.5 I	30.9	1750 ± 100	2350	1.343	$-5.67^{+0.18}_{-0.19}$	H	−5.92	−0.25
152424	O9.5 I	30.9	1760	2200	1.250	$-5.26^{+0.17}_{-0.17}$	R	−5.69	−0.43
37128	B0 Ia	28.0	1500 ± 150	2110	1.407	$-5.39^{+0.16}_{-0.16}$	R	−5.91:	−0.52
mean					1.39 ± 0.05				-0.41 ± 0.05
std. dev.					0.20				0.18
				Class II and III					
15558	O5 III	42.3	3350 ± 200	3590	1.072	$-5.61^{+0.19}_{-0.23}$	H	−5.69	−0.08
190864	O6.5 III	39.2	2450 ± 150	3590	1.465	$-5.88^{+0.18}_{-0.20}$	H	−6.21	−0.33
24912	O7.5 III	37.1	2400 ± 100	3520	1.467	$-5.89^{+0.18}_{-0.19}$	H	−6.52	−0.63
36861	O8 III	36.0	2400 ± 150	3410	1.420	$-6.20^{+0.21}_{-0.41}$	H	−6.51	−0.31
37043	O9 III	34.0	2450 ± 150	2960	1.208	$-6.50^{+0.18}_{-0.18}$	R	−6.23	+0.27
57061	O9 II	34.0	1960	2560	1.306	$-5.20^{+0.15}_{-0.15}$	R	−5.62	−0.42
36486	O9.5 II	32.9	2000	2490	1.245	$-5.97^{+0.15}_{-0.15}$	R	−5.87	+0.10
mean					1.31 ± 0.06				-0.20 ± 0.13
std. dev.					0.15				0.31
				Class V					
46223	O4 V	46.4	2800 ± 60	4550	1.625	$-5.85^{+0.18}_{-0.20}$	H	−6.15	−0.30
164794	O4 V	46.4	2950 ± 150	4060	1.376	$-5.62^{+0.19}_{-0.20}$	H	−5.70	−0.08
15629	O5 V	44.3	2900 ± 70	4120	1.421	$-5.77^{+0.18}_{-0.20}$	H	−6.07	−0.30
46150	O5 V	44.3	2900 ± 200	4110	1.417	< -5.88	H	−6.06	
47839	O7 V	40.1	2300 ± 200	4040	1.757	$-6.30^{+0.21}_{-0.41}$	H	−6.58	−0.28
149757	O9 V	35.9	1500 :	3920		$-7.41^{+0.16}_{-0.16}$	R	−7.05	+0.36
mean					1.52 ± 0.08				-0.12 ± 0.14
std. dev.					0.16				0.28

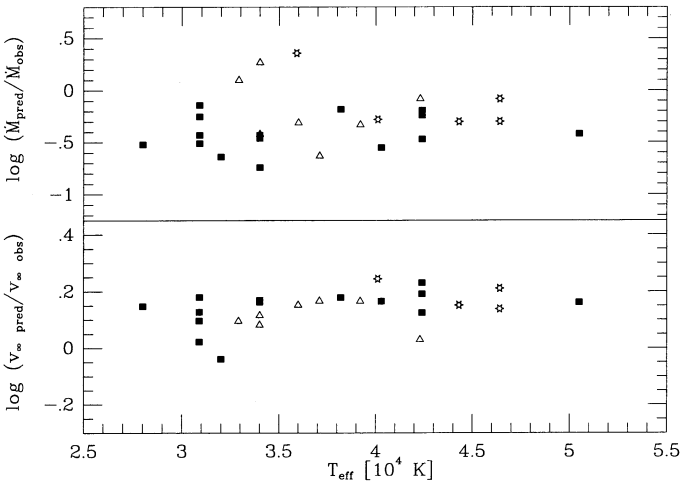

FIG. 5.—Logarithmic differences between observed and theoretical mass-loss rates and terminal velocity vs. $T_{\rm eff}$. *Solid squares:* supergiants; *asterisks:* giants and bright giants; *open triangles:* dwarfs. The figure includes all stars having entries in Table 7.

logarithmic differences as a function of $T_{\rm eff}$ in Figure 5. This figure shows that there is no trend between the differences and $T_{\rm eff}$.

We have also plotted the differences versus the mean density $\langle\rho\rangle$ in the wind, defined by equation (6). There is no indication for a relation between $v_{\infty\ \rm pred}/v_{\infty\ \rm obs}$ and $\langle\rho\rangle$. (This figure is not shown here.) However, Figure 6 shows that the ratio $\dot{M}_{\rm pred}/\dot{M}_{\rm obs}$ does show a clear trend with $\langle\rho\rangle$ in the sense that $\log(\dot{M}_{\rm pred}/\dot{M}_{\rm obs})$ is approximately 0 at low densities, but decreases if the wind density increases. The least-squares fit through the data give the following relation:

$$\log \frac{\dot{M}_{\rm pred}}{\dot{M}_{\rm obs}} = -0.61 - 0.59 \log (10^{13}\ \langle\rho\rangle)\ . \qquad (20)$$

This relation, which is also plotted in Figure 6, is valid in the range of $-14.5 < \log(\langle\rho\rangle) < -12.5$. The data points scatter around this relation within 0.2 dex. Such a scatter is expected from the uncertainties in the observed and predicted mass-loss

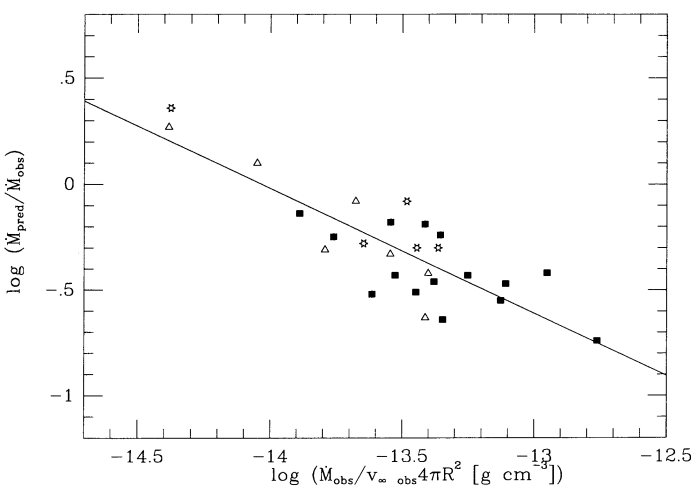

FIG. 6.—Logarithmic differences between observed and theoretical mass-loss rates vs. mean wind density. The solid line is the least-squares fit given by eq. (20). Symbols are as in Fig. 5. The differences become larger for higher wind densities.

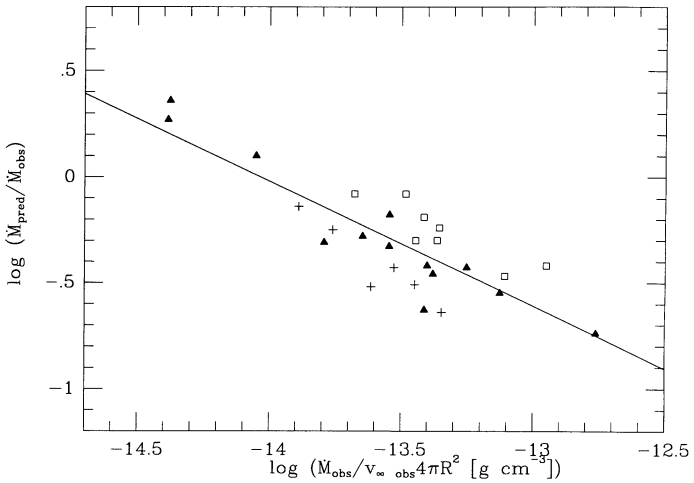

FIG. 7.—Logarithmic differences between observed and theoretical mass-loss rates vs. mean wind density. As in Fig. 6, the solid line is the least-squares fit given by eq. (20). Different symbols denote different temperature ranges. *Crosses:* $T_{\rm eff} < 32{,}500$ K; *solid triangles:* $32{,}500\ {\rm K} \le T_{\rm eff} < 42{,}000$ K; *open squares:* $T_{\rm eff} > 42{,}500$ K.

rates rates. In the density region of $-13.8 < \log(\langle\rho\rangle) < -13.3$, which contains stars of all luminosity classes, there is no systematic difference between the different luminosity classes. There is however a trend with temperature. This is shown in Figure 7, where we have used different symbols to indicate three temperature ranges of $T_{\rm eff} < 32{,}500$ K, $32{,}500\ {\rm K} \le T_{\rm eff} < 42{,}000$ K, and $T_{\rm eff} > 42{,}500$ K. This figure shows the general trend that the hotter stars fall on the average above the mean relation by about 0.10 dex and the cooler stars fall on the average below the mean relation by 0.10 dex. (We will use this result later to derive accurate predictions of mass-loss rates as a function of the stellar parameters.) In § 6.1 we argued that the adopted mean values of the force multiplier parameters may result in an *overestimate* of the mass-loss rates for stars with $T_{\rm eff} < 33{,}000$ K by about a factor of 2. This implies that the discrepancy between predictions and observations would even have been larger for these stars if we had adopted the lower value of k, suggested by Pauldrach et al. (1990).

We also argued in § 6.1 that the value of k might be overestimated if our program stars have abundances closer to the Orion stars than to the solar abundances. This would have resulted in a further downward shift of all points in Figures 6 and 7.

6.4. *Inclusion of WNL Stars*

Bohannan (1990) demonstrated that there exists a smooth progression of quantitative spectroscopic properties from Of stars, via Ofpe/WNL stars, to classical WNL stars. WNL stars are generally considered to be less evolved Wolf-Rayet stars (Maeder 1990). Some hydrogen is still left in the atmospheres of the coolest ($T_{\rm eff} \approx 30{,}000$ K) WN stars (Hamann 1991), suggesting an evolutionary relation with very luminous Of supergiants, which exhibit helium overabundances relative to main-sequence stars (cf. Table 1). Studies of the spectral morphology in the optical (Walborn 1974) and ultraviolet (Walborn et al. 1985) spectral regions may suggest that Of, Ofpe/WNL, and WNL stars form a sequence of increasing wind density. We showed in the previous section that the discrepancy between observed and predicted mass-loss rates among O stars increases with increasing wind density. Since

WNL stars have even higher wind densities, we expect that the trend found in Figure 6 is preserved if WNL stars are added to the sample.

The theory of radiatively driven winds in its present version cannot account for the observed mass-loss rates of Wolf-Rayet stars (Cassinelli 1991). Essentially, this is due to the observed efficiency

$$\eta = \frac{\dot{M} v_\infty}{L/c} \tag{21}$$

of the momentum transfer in Wolf-Rayet winds which is typically more than an order of magnitude higher than what is expected for complete conversion of radiative into kinetic momentum. WNL stars are less extreme in this respect, with η between 1 and 10. For instance, Schmutz et al. (1991) found in a detailed analysis of the Ofpe/WNL star R84 $\eta \approx 1$–2. One should be aware that the theory of radiatively driven winds cannot be expected to provide quantitative wind properties of WNL stars. However, application of the wind models to WNL stars with their relatively weak Wolf-Rayet winds and comparison to extreme Of stars may help to gain insight into the reason for the breakdown of the theory when applied to very luminous O stars.

We adopted a sample of eight WNL stars with well-determined stellar parameters published by Schmutz, Hamann, & Wessolowski (1989). They are listed in Table 8. $T_{\rm eff}$ refers to the temperature at the radius where the Rosseland optical depth equals 2/3. The effective temperatures of all eight stars are around 30,000 K. The bolometric luminosities, mass-loss rates, and terminal velocities were obtained from a comprehensive non–LTE analysis of the optical helium spectrum. Masses of single WNL stars are generally not very well known. Cherepashchuk (1991) finds an average mass of 20 $M_\odot$ for WNL stars in binaries. We assume that this value is also representative for our sample of WNL stars. Support for this value of M comes from a recent non–LTE analysis of a large sample of Wolf-Rayet stars (Hamann, Koesterke, & Wessolowski 1993), which includes all eight WNL stars of Table 8. Luminosities were derived from optical spectra and masses assigned via a mass-luminosity relation for bare helium cores. The mean mass of the WNL stars in Table 8 turns out to be $23 \pm 4\ M_\odot$. Even if the actual masses were different from what we adopted, our main conclusion would be unchanged. Below we will demonstrate that there also exists a *momentum discrepancy*, and this discrepancy does not depend on the stellar mass.

Following Nugis (1991) we adopt N(He)/N(H) abundance ratios of 0.5, 1, and 2 for spectral type WN9, WN8, and WN7, respectively. Helium is assumed to be fully ionized. Using these

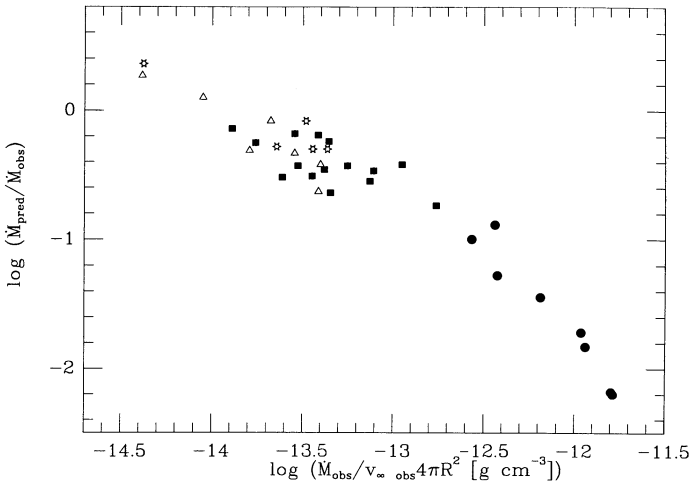

FIG. 8.—Logarithmic differences between observed and theoretical mass-loss rates vs. mean wind density. This figure is an extension of Fig. 6 by including a sample of WNL stars. *Solid circles:* WNL stars. Other symbols are as in Fig. 5.

model parameters we can predict theoretical mass-loss rates for the WNL stars as we did for the O star sample. The results are listed in Table 8. As expected, $\dot{M}_{\rm pred}$ is much lower than $\dot{M}_{\rm obs}$. $\dot{M}_{\rm pred}/\dot{M}_{\rm obs}$ versus $\langle\rho\rangle$ is plotted for all eight WNL stars and the entire O star sample in Figure 8. It is evident that the WNL stars extend the relation which had been found in Figure 6 toward higher wind densities. We note that there is no abrupt discontinuity in the relation at the borderline between Wolf-Rayet and O stars. Rather, the most extreme Of star (HD 152408) has a value of $\dot{M}_{\rm pred}/\dot{M}_{\rm obs}$ which is similar to those of the least extreme Wolf-Rayet stars. We interpret this result as a confirmation of the suggestion that the theory of radiatively driven winds in its present formulation underestimates $\dot{M}$ of O stars, and that the disagreement depends on the wind density.

The reason for the failure of the wind theory when applied to Wolf-Rayet stars is the high efficiency of momentum transfer in Wolf-Rayet winds. In Figure 9 we show the logarithmic ratio of the theoretical and predicted momentum flux $(\dot{M}_{\rm pred}\, v_{\infty\ \rm pred})/(\dot{M}_{\rm obs}\, v_{\infty\ \rm obs})$ versus η as defined by equation (21). The efficiency factors derived for the most massive O star winds are close to—or even above—1. $(\dot{M}_{\rm pred}\, v_{\infty\ \rm pred})/(\dot{M}_{\rm obs}\, v_{\infty\ \rm obs})$ of the O star and W-R star sample displays a very tight correlation with η. O stars and WNL stars form a homogeneous sample in their values of $(\dot{M}_{\rm pred}\, v_{\infty\ \rm pred})/(\dot{M}_{\rm obs}\, v_{\infty\ \rm obs})$ when plotted versus η. We conclude from this figure that the breakdown of the wind theory, which is apparent in the case of Wolf-Rayet stars, already exists—with much less dramatic consequences—in

TABLE 8

PARAMETERS OF WNL STARS

WR	Spectral Type	T_{eff} [K]	log L [$L_\odot$]	$v_{\infty\ obs}$ [$km\ s^{-1}$]	log $\dot{M}_{obs}$ [$M_\odot yr^{-1}$]	log $\dot{M}_{pred}$ [$M_\odot yr^{-1}$]	log $\frac{\dot{M}_{pred}}{\dot{M}_{obs}}$
25	WN7	35,000	5.7	1200	−4.9	−5.90	−1.00
24	WN7	32,000	5.7	1200	−4.6	−5.88	−1.28
22	WN7	32,000	5.9	1000	−4.5	−5.39	−0.89
78	WN7	31,000	5.8	1200	−4.2	−5.65	−1.45
16	WN8	31,000	5.5	900	−4.4	−6.23	−1.83
40	WN8	28,000	5.4	1000	−4.2	−6.40	−2.20
105	WN8	30,000	5.7	900	−4.1	−5.82	−1.72
108	WN9	30,000	5.1	900	−4.7	−6.88	−2.18

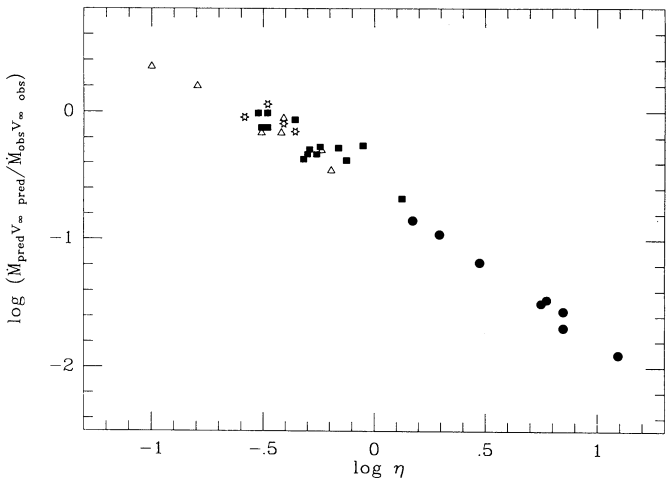

FIG. 9.—Logarithmic differences between observed and theoretical momentum fluxes vs. efficiency factor η. $\dot{M}_{obs}$ and $v_{\infty\ obs}$ were used to calculate η. O stars with the highest mass-loss rates have efficiency factors of order unity and form a natural extension of WNL stars. The meaning of the symbols is as in Fig. 8.

very dense O star winds. These results suggest that the ultimate reason for the $\dot{M}$ (and probably the v_∞) discrepancy in O stars is the insufficient treatment of the momentum transfer from the radiation field to the stellar wind in the theory.

If the abundances of the O stars are closer to those of the Orion stars than to those of the Sun (see § 6.1) the points in Figure 9 should be shifted further downwards. In that case, the data in Figures 6 and 9 suggest that the predicted mass-loss rates and momentum fluxes of the O stars with low-density winds or with small values of $(\dot{M}_{obs} v_{\infty\ obs})/(L/c)$ are correctly predicted by the radiation driven wind models but that the discrepancy increases to higher density winds.

7. THE ORIGIN OF THE DISCREPANCIES

The data presented in Figures 5–9 and in Table 7 showed that the predicted terminal velocities of the O stars are about a factor 1.4 higher than observed and the predicted mass-loss rates are too low by up to a factor 0.25, depending on the density in the wind. In this section we will consider the possible origin of these discrepancies. Two possibilities will be investigated: errors in the adopted stellar parameters and errors in the radiation-driven wind theory.

7.1. *Errors in the Stellar Parameters*

In this section we assume that the stellar wind theory and the adopted values of k, α, and δ are correct and that the discrepancies in $v_{\infty\ pred}$ and $\dot{M}_{pred}$ can be blamed on errors in the adopted stellar parameters.

7.1.1. *Errors in the Distances and Radii?*

The predicted value of v_∞ is proportional to v_{esc} with a proportionality factor that depends on α and δ (Abbott 1982; Pauldrach et al. 1986). Thus the discrepancy in v_∞ could be solved by reducing our adopted value for v_{esc} by about a factor of 0.7, which corresponds to reduction of the value of M/R by a factor of 0.5. The values of R adopted in this paper have been derived from L and T_{eff}. The values of T_{eff} are based on non–LTE studies of the energy distributions and line ratios of a set of O stars. These values are probably correct within about 5% (Herrero et al. 1992 and § 2). The radius follows from L and T_{eff} or from M_V and T_{eff}. Most of our program stars are in clusters with well-determined distances. In order to reduce the value of v_{esc} by a factor of 0.7, we would have to assume that the cluster distances are systematically too small by a huge factor since, to first order, v_{esc} does not depend on the distance. For instance, increasing the distance by some factor increases R by the same factor. The mass of the star, derived from T_{eff}, L and the evolutionary tracks would also increase by this factor, since $M \propto L^{1/2}$, and so v_{esc} would be independent of the distance.

7.1.2. *Errors in the Stellar Masses?*

The alternative explanation of the discrepancies of v_∞ and $\dot{M}$ would be the assumption that the adopted masses of the stars, derived from the evolutionary tracks are wrong. This was one of the possibilities suggested by Groenewegen et al. (1989) to explain the low observed values of v_∞. This suggestion seems to be supported by the low spectroscopic gravities of the O stars, derived from fitting of line profiles and line ratios by Herrero et al. (1992). Typically, the masses derived from the spectroscopic gravities are lower by about a factor of 0.6–0.8 than derived from evolution theory, but the dispersion is large.

A decrease of M would result in a decrease of v_∞ and an increase of $\dot{M}$ because v_{esc} and g_{eff} would be smaller. We have derived the dependence of v_∞ and $\dot{M}$ on M by calculating these values with the method described in § 6.1 for nine program stars of different spectral types and luminosity classes. These stars and their values of $d \log \dot{M}/d \log M$ and $d \log v_\infty/d \log M$ are listed in Table 9. The gradients were derived by decreasing M by 0.1 dex. For a decrease in M of 0.2 dex the gradients are slightly higher because $\dot{M}$ and v_∞ are not strictly linear with M. In Table 9 we also give the values of $\log L/M$ in solar units because both $\dot{M}$ and v_∞ are expected to depend on it.

The data in this table show that $v_{\infty\ pred}$ decreases and $\dot{M}$ increases with decreasing M. Notice that in Table 9 the gradients $d \log \dot{M}/d \log M$ and $d \log v_\infty/d \log M$ are very similar

TABLE 9

DEPENDENCE OF $v_{\infty\ pred}$ AND $\dot{M}_{pred}$ ON THE ADOPTED STELLAR MASS AND ON k, α, AND δ

HD	Spectral Type	$\log \frac{L}{M}$	$\frac{d \log v_\infty}{d \log M}$	$\frac{d \log \dot{M}}{d \log M}$	$\frac{d \log \dot{M}}{d \log k}$	$\frac{d \log \dot{M}}{d \log \alpha}$	$\frac{d \log \dot{M}}{d \log \delta}$	$\frac{d \log v_\infty}{d \log \alpha}$	$\frac{d \log v_\infty}{d \log \delta}$
66811	O4 If	4.13	+0.94	−0.96	+1.03	+5.34	+0.55	+1.79	−1.20
151804	O8 I	4.30	+1.53	−1.58	+1.05	+4.91	−0.10	+1.46	−0.30
30614	O9.5 I	4.15	+1.12	−1.14	+1.03	+5.62	−0.80	+1.53	−0.25
15558	O5 III	4.19	+1.16	−1.18	+1.03	+5.05	+0.70	+1.79	−1.25
36861	O8 III	3.89	+0.77	−0.80	+1.04	+6.23	+0.00	+1.79	−1.20
36486	O9.5 II	4.17	+1.17	−1.18	+1.03	+5.50	−0.70	+1.57	−0.25
46223	O4 V	3.98	+0.70	−0.74	+1.03	+5.76	+0.60	+1.79	−1.20
47839	O7 V	3.82	+0.66	−0.69	+1.04	+6.30	+0.20	+1.79	−1.25
149757	O9 V	3.62	+0.57	−0.61	+1.04	+7.12	−0.40	+1.79	−1.20

except for the different sign in all cases. This means that the predicted momentum of the wind, $\dot{M}v_\infty$, is invariant to small changes, $\lesssim 0.2$ dex, in the assumed mass. The reason for this is simply that in the radiation-driven wind models the amount of momentum transferred from the radiation to the gas is almost independent of the stellar mass. We may thus expect that the predicted *momentum loss* of the wind is equal to the observed value if the observed discrepancies are due to errors in the adopted masses.

In Figure 10 we show the observed and predicted values of the wind momentum versus the radiative momentum loss of the star. The predicted wind momentum shows a rather strict correlation with L/c.

$$\log\,(10^{-29}\,\dot{M}_{\rm pred}\,v_{\infty\,\rm pred}) = -0.54 + 1.27\,\log\left(10^{-29}\,\frac{L}{c}\right), \tag{22}$$

with an uncertainty of only 0.1 in the range $28 < \log L/c < 29.5$. This means that the predicted efficiency of momentum transfer from radiation to the wind for our program stars is

$$\eta_{\rm pred} = 0.308\left(10^{-6}\,\frac{L}{L_\odot}\right)^{0.27}, \tag{23}$$

within 0.1 dex. The observed momentum of the O star winds is on the average 0.17 ± 0.04 higher than predicted and does not strictly correlate with L/c (see Fig. 10*a*). This is not surprising since we showed earlier in Figure 8 that the ratio between $\dot{M}_{\rm pred}$ and $\dot{M}_{\rm obs}$ depends on the density of the wind. The observed momentum of the winds of the WNL stars is much larger than predicted. It is even larger than L/c.

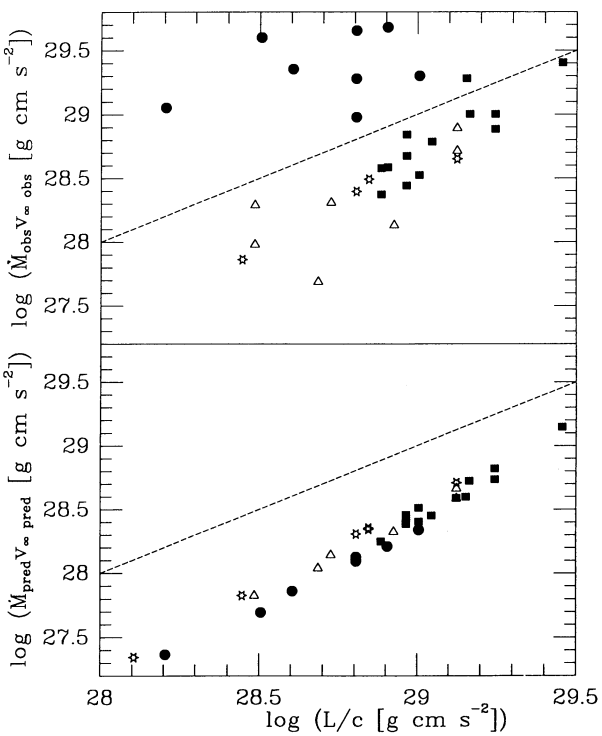

FIG. 10.—Observed (*upper part*) and theoretical momentum flux of the wind versus L/c. The dashed line indicates an efficiency factor η of unity. The meaning of the symbols is as in Fig. 8. The predicted momentum flux for all stellar types is tightly correlated with L/c (see eq. [22]). The observed momentum flux is higher on average than the theoretical prediction. The discrepancy is largest for supergiants and WNL stars.

We conclude that the discrepancy between the observed and predicted mass-loss rates of the O stars cannot be explained by adopting a smaller mass for the O stars since the predicted and observed *momentum* of the wind show a similar discrepancy, independent of the adopted stellar mass.

7.2. *Errors in the Radiation-Driven Wind Theory?*

In this section we assume that the adopted stellar parameters are correct and that the discrepancy in $v_{\infty\,\rm pred}$ and $\dot{M}_{\rm pred}$ are due to errors in the radiation driven wind models.

7.2.1. *Errors in the Force Multiplier Parameters k, α, and δ?*

The dependence of $\dot{M}_{\rm pred}$ and $v_{\infty\,\rm pred}$ on k, α, and δ were calculated for the nine program stars of Table 9. The gradients were calculated for $\Delta k = +0.03$, $\Delta\alpha = -0.1$, and $\Delta\delta = +0.02$. These values were chosen because they are expected to increase $\dot{M}_{\rm pred}$ and decrease $v_{\infty\,\rm pred}$. The results are listed in Table 9. This table shows a reduction of $v_{\infty\,\rm pred}$ and an increase in $\dot{M}_{\rm pred}$ cannot be reached by changing only one of the force multiplier parameters. A decrease of $v_{\infty\,\rm pred}$ by a factor of 0.7 ($= -0.15$ dex) could be achieved by assuming a reduction in α from the adopted value of 0.693–0.602. This would result in a *decrease* of $\dot{M}_{\rm pred}$ by about -0.5 dex, so the value of k has to be increased drastically (by about 0.5) to compensate the decrease of $\dot{M}_{\rm pred}$ produced by α and by an additional term to increase $\dot{M}_{\rm pred}$ to reach the observed values.

A reduction in $v_{\infty\,\rm pred}$ by 0.15 dex could also be achieved by increasing the value of δ from 0.056 to about 0.2. This would also increase $\dot{M}_{\rm pred}$ of the hot O stars with $T_{\rm eff} > 36{,}000$ K and decrease $\dot{M}_{\rm pred}$ of the cooler O stars by factors of about 0.1 or so. An increase of $\dot{M}_{\rm pred}$ to match the observed values would still require an increase in k which would amount to about 0.7 for the most discrepant O star. This is large compared to the nominal value of 0.052.

Combinations of changes in α and δ are also possible, of course. However, they all require a significant increase of k to explain the observed mass-loss rates.

Here we should remember that the adopted values of the force multipliers are based on the calculations for solar composition. If the metallicity of the O stars is closer to that of the Orion Nebula and of the Orion stars, then the value of k and $\dot{M}_{\rm pred}$ would even be smaller than adopted.

7.2.2. *Changes in the Properties of the Driving Lines?*

Suppose that the radiation-driven wind models are in principle correct and that the discrepancy between the observed and predicted mass-loss rates and terminal velocities is due only to errors in the calculations of the force multipliers. In that case we have to explain what the cause of these errors is. A drastic increase in the value of k needed to explain the observed values of $\dot{M}$ would indicate that there are many more driving lines than predicted, or that the driving lines are more efficient in transferring radiative momentum into the wind.

The discrepancy between the predicted and observed mass-loss rates or momentum of the wind might be due to errors in the predicted degree of ionization in the winds of O stars. This might change the nature and efficiency of the lines that drive the wind. Groenewegen & Lamers (1991) have shown that the empirical ionization fractions derived from observed UV lines can differ drastically from those predicted by Pauldrach et al. (1990) by factors up to 10 or more. This is probably due to the fact that the radiation-driven wind models are calculated with

a constant wind temperature of $T_{\rm wind} = T_{\rm eff}$ and neglect the effects of shocks which produce the well-known super-ionization and the observed X-ray fluxes (Cassinelli et al. 1981; Lucy & White 1980; Owocki 1992 and references therein).

The effect of errors in the predicted degree of ionization in the wind on the predicted mass-loss rate and wind momentum can be very large. This has been shown recently by Lucy & Abbott (1993) who found that the observed decrease of ionization with distance in the winds of WR stars significantly increases the efficiency of transfer of radiative momentum into the wind by multiple scattering compared to predictions with constant ionization. In their example they found that the wind momentum can exceed the momentum of the single scattering limit by factors of the order of 10! ($\eta = 10$ in eq. [21]). The smooth continuation of the discrepancy from O stars to WNL stars in Figures 8 and 9 suggests that the same mechanism that is responsible for the discrepancy in the WNL stars is also responsible for the (smaller) discrepancy in the O stars. So if the discrepancy of the WNL stars is solved by taking into account the decreasing ionization, the same effect might solve the discrepancy of the O stars. In that case it is not surprising that we found a relation between the discrepancy and the mean density in the wind (Figs. 6–8) because the ionization is expected to be sensitive to the density in the winds through the optical depths of the ionizing continua.

8. MASS LOSS AND EVOLUTION

We studied the dependence of the observed mass-loss rates on stellar parameters. Multi-dimensional fits for $\dot{M}$ as a function of L, $T_{\rm eff}$, R, and M are inconclusive with respect to the question which parameters ultimately affect the mass-loss rates. Stellar evolution models require $\dot{M}$ parameterized in terms of L and $T_{\rm eff}$. Therefore we give a fitting formula for $\dot{M}$ as a function of these two stellar parameters:

$$\log \dot{M} = 1.738 \log L - 1.352 \log T_{\rm eff} - 9.547 \qquad (24)$$

($\dot{M}$ in $M_\odot$ yr^{-1}, L in $L_\odot$, $T_{\rm eff}$ in K). This relation is valid for $5.0 < \log L < 6.4$ and $4.45 < \log T_{\rm eff} < 4.70$. The standard deviation of individual mass-loss rates from equation (24) is $\sigma = 0.23$. This is comparable to the observational uncertainties suggesting that the accuracy of equation (24) is predominantly limited by the errors associated with the derived mass-loss rates and not by additional functional dependencies on other stellar parameters, which are not included in this fitting relation. Figure 11 is a comparison of the mass-loss rates derived observationally (from Table 7) and calculated with equation (24). The fitting formula reproduces the observed mass-loss rates over approximately two orders of magnitude. It is particularly well-determined at the high-$\dot{M}$ end, where many observational data points are available. Conversely, the mass-loss regime below $10^{-7}\ M_\odot$ yr^{-1} is represented by one data point only and should be taken with care. We compared equation (24) to the mass-loss versus luminosity relation

$$\log \dot{M} = -6.87 + 1.62 \log L \qquad (25)$$

published by Garmany & Conti (1984) ($\dot{M}$ in $M_\odot$ yr^{-1}, L in $10^5\ L_\odot$). There is no significant difference between the predictions of the two relations for the 27 stars of Table 7: $\log \dot{M}$(eq. [24]) $-$ $\log \dot{M}$(eq. [25]) $= -0.07 \pm 0.09$. Garmany & Conti (1984) derived their relation from a sample of O stars with ultraviolet mass-loss rates. However, it should be realized that the agreement between equations (24) and (25) does not prove

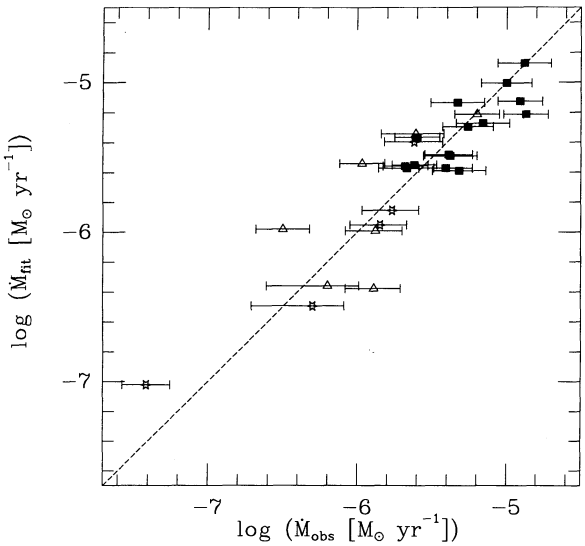

FIG. 11.—$\dot{M}$ predicted by the fitting formula eq. (24) vs. observed mass-loss rates. Symbols are as in Fig. 5. Error bars refer to the observational errors.

that ultraviolet mass-loss rates have no systematic offset relative to Hα and radio data. Garmany & Conti had to increase their original sample of program stars with stars having radio mass-loss rates and with the sample of Garmany et al. (1981) in order to achieve meaningful statistics. In principle, Garmany et al. (1981) used ultraviolet resonance lines to derive $\dot{M}$. In practice, however, they scaled their rates with a factor derived from a comparison with the radio mass-loss rate of ζ Puppis so that *ultimately the rates published by Garmany et al. (1981) are heavily biased toward radio data.* Therefore the agreement between equations (24) and (25) simply demonstrates the consistency of different radio mass-loss rates. Howarth & Prinja (1989) studied the mass-loss properties of a large sample of O stars and derived

$$\log \dot{M} = 1.69 \log L - 15.4\ , \qquad (26)$$

where $\dot{M}$ is in $M_\odot$ yr^{-1} and L in $L_\odot$. This relation is based on ultraviolet data which were scaled to radio mass-loss rates in order to bypass the problem of the uncertain ionization conditions in the winds. We compared the mass-loss rates of equation (24) to those following from equation (26) and found $\log \dot{M}$(eq. [24]) $-$ $\log \dot{M}$(eq. [26]) $= -0.05 \pm 0.09$. As in the case of equation (25), we find that our fitting relation is consistent with mass-loss predictions derived by other methods. However, it must be emphasized again that equation (24) as well as equation (26) are not independent but rely predominantly on radio data.

Stellar evolution models commonly adopt the mass-loss parameterization published by de Jager, Nieuwenhuijzen, & van der Hucht (1988); see, for instance, Maeder (1990). This parameterization gives $\dot{M}$ in terms of L and $T_{\rm eff}$ across the entire Hertzsprung-Russell diagram. Since stellar evolution is crucially dependent on $\dot{M}$, any revisions to the mass-loss parameterization has significant consequences for evolutionary models. We calculated $\dot{M}$ from equation (24) for each evolutionary model of Maeder (1990) having parameters $\log L > 5.0$ and $\log T_{\rm eff} > 4.45$. This corresponds to the valid parameter range of equation (24). Stars in the Wolf-Rayet phases have been excluded. In Figure 12 we show the total mass which is lost as a function of stellar age. Tracks with initial masses of

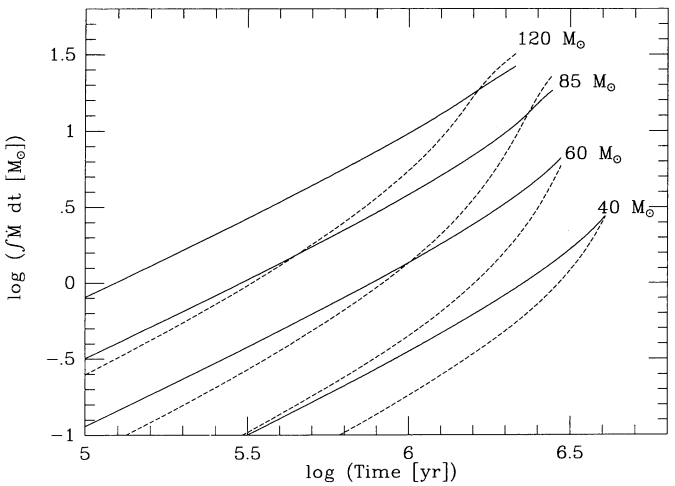

FIG. 12.—Total mass lost during main-sequence and early post–main-sequence evolution. The dashed lines were calculated using Maeder's (1990) mass-loss rates for stars with solar composition. The solid lines are based on eq. (24), with Maeder's stellar parameters as input. The four sets of curves refer to zero-age main-sequence masses of 120 $M_\odot$, 85 $M_\odot$, 60 $M_\odot$, and 40 $M_\odot$.

120 $M_\odot$, 85 $M_\odot$, 60 $M_\odot$, and 40 $M_\odot$ are considered. The two curves for each track correspond to Maeder's tabulated values (based on de Jager's formula) and to the prediction of equation (24). Our mass-loss formula predicts somewhat higher mass loss during early main-sequence evolution and slightly lower values during later phases. The endpoints of the curves in Figure 12 are dictated by the requirements $\log T_{\rm eff} > 4.45$ and the stars not being in the Wolf-Rayet phase. At the end of the evolutionary phases covered in Figure 12, equation (24) and de Jager's parameterization predict about the same total mass lost due to stellar winds.

9. DISCUSSION AND SUMMARY

We have derived the mass-loss rates of 27 O stars and one B0 supergiant from radio observations (§ 3) and Hα emission (§ 4) using accurate determinations of the terminal velocities and of the velocity laws based on detailed fitting of UV resonance lines by Groenewegen & Lamers (1989). For the 14 stars for which $\dot{M}$ could be derived by both methods, the two determinations of the mass-loss rates agree within 0.03 ± 0.23 dex (§ 5). The excellent agreement between the two sets suggests that clumping due to shocks in the wind does not seriously affect the mass-loss determinations because clumping is expected to depend on the distance from the star while Hα and radio fluxes are formed at different distances.

The derived mass-loss rates and the terminal velocities are compared with the predictions of the radiation-driven wind theory, using the force multiplier parameters of Pauldrach et al. (1990) (§ 6). For the full sample of program stars, the predicted terminal velocities are higher than observed by a factor of 1.4, and the predicted mass-loss rates are smaller than observed by -0.29 ± 0.26 dex. The discrepancy between theoretical and observed mass-loss rates for stars having luminosity classes II–V is less severe (and may not even be statistically significant). For the subset of supergiant stars, however, we find a significant discrepancy of -0.41 ± 0.18 dex.

We found that the ratio between predicted and observed mass-loss rates does not depend on $T_{\rm eff}$ but that it shows a strong correlation with the mean density in the wind: the higher the mean density, the larger the discrepancy (eq. [20] and Figs. 6 and 7). The force multiplier parameters which describe the radiation pressure due to numerous lines were calculated with the assumption of solar abundances. Recent studies have shown that the oxygen abundance of stars in Orion are smaller than in the Sun. If these smaller abundances had been adopted in the calculations of the radiation-driven wind models, the predicted mass-loss rates would even have been smaller and the discrepancy between predicted and observed mass-loss rates would have been higher.

We included eight Wolf-Rayet stars of types WNL in our sample. These stars have spectroscopically similar characteristics as the O stars and seem to form a natural evolutionary sequence with the Of stars. The relation between $\dot{M}_{\rm pred}/\dot{M}_{\rm obs}$ and the mean wind density extends from the O stars into the WNL stars (Fig. 8). This suggests that the mechanism which is responsible for the high mass-loss rates and the large momentum of the winds of WNL stars is already operating in the winds of O stars. Lucy & Abbott (1993) have shown that the momentum problem of the winds of WR stars can be resolved by taking into account the gradient in the degree of ionization through the wind. In that case, multiple scattering of photons can occur over much larger distances in the wind. This makes the transfer of momentum from the radiation to the gas much more efficient and results in a wind momentum above the single-scattering limit of $\eta = \dot{M} v_\infty/(L/c) = 1$. Our observations suggest that this effect is also responsible for the fact that the observed mass-loss rates in O stars are higher than predicted because the discrepancy follows the same trend with density in the O stars as in the WNL stars.

At first sight our results seem to be in contradiction with those of Pauldrach et al. (1990) and Kudritzki et al. (1992) who find that the observed mass-loss rates and terminal velocity are in excellent agreement with the predictions from the radiation-driven wind theory. This agreement, however, is due to the fact that these authors adopted stellar masses, derived from spectroscopic gravities, which are considerably smaller than those derived from evolutionary tracks. The most drastic example is the star P Cygni, for which Pauldrach & Puls (1990) derive a mass of only 23 ± 2 $M_\odot$ to explain the mass-loss rate and the wind velocity. At such a low mass, a star with the luminosity of P Cygni, $\log L = 5.9$, would have lost all of its H envelope and would be a WR star if the predictions of stellar evolution theory are correct. We have shown in § 7.1 that the reduction of the mass cannot solve the discrepancy between observations and theory because the observed momentum of the winds of O stars is higher than predicted (Figs. 9 and 10), and the predicted momentum of the wind is almost independent of the adopted stellar mass (§ 7.1.2). Therefore we conclude that the discrepancy between predicted and observed mass-loss rates, terminal velocities, and wind momentum cannot be solved by assuming smaller masses of the stars.

This leaves the question of the low *spectroscopic* masses of the O stars unanswered. In principle, the spectroscopic and the v_∞ method are independent, and they both hint at stellar masses which are on average lower than those based on stellar evolution theory. Our results suggest that the prediction of the radiatively driven wind theory may not be correct for the most luminous O stars and that stellar masses derived from v_∞ may be affected by this. *However, we emphasize that our results do not exclude that evolutionary masses are incorrect. Rather, we find that the momentum discrepancy is independent of M.* Spectroscopic and evolutionary masses could be reconciled if the values of $\log g$ derived from non–LTE analyses were system-

atically underestimated by about 40%, i.e., by 0.15 in log g. As an example, Bohannan et al. (1990) derived log $g = 3.50 \pm 0.1$ from their spectroscopic analysis of HD 66811, whereas the evolutionary masses require a gravity which is higher by about 0.3 dex. The discrepancy can partly be explained by wind contamination of photospheric absorption lines used for the non–LTE analysis. In fact, a recent redetermination of the log g value of HD 66811 (R. P. Kudritzki, private communication) with a "unified" model suggests log $g \approx 3.65$, which results in a spectroscopic mass closer to the evolutionary value. However, this does not yet solve the full problem, and more work is clearly needed.

The mass-loss rates derived in this paper can be expressed in terms of a fitting formula as function of L and $T_{\rm eff}$ (eq. [24]). The mass-loss rates predicted by this formula are higher than according to the parameterization by de Jager et al. (1988) at the beginning of the main sequence but drop below the predictions by de Jager at the end of the main sequence. The total mass lost during the main sequence according to equation (24) and de Jager et al. are about the same (Fig. 10). This difference in the time dependence of the mass-loss rates of O stars may have consequences for the structure of circumstellar shells and bubbles around massive stars.

The mass-loss rates derived in this paper agree reasonably well with those used by Maeder (1990) in the calculation of the evolutionary tracks of massive stars. The agreement between the predicted and observed properties in the stars in the upper H-R diagram (Maeder 1990) gives additional support for the validity of the derived mass-loss rates. Since our mass-loss rates are typically higher by a factor of 2 than the values predicted by the radiation-driven wind theory, stellar evolution models would be significantly affected if the theoretical values were adopted. This same conclusion was reached by El Eid & Hartmann (1993) on the basis of detailed evolutionary calculations for P Cygni. They were able to model the observed brightness evolution of P Cygni (Lamers & de Groot 1992) only if they adopted de Jager et al.'s mass-loss formula (which is similar to our results) but not with the prediction of the radiation-driven wind theory.

H. J. G. L. M. L. gratefully acknowledges the kind hospitality of STScI where most of this research was done. We thank I. Howarth and A. Brown for providing us their new determinations of the radio fluxes at 3.6 cm and E. Schuiling for preliminary investigations that triggered this study. Helpful comments by W.-R. Hamann, A. Herrero, I. Howarth, W. Schmutz, N. Walborn, and the referee R. Kudritzki improved this paper.

REFERENCES

Abbott, D. C. 1982, ApJ, 259, 282
Abbott, D. C., Bieging, J. H., & Churchwell, E. 1981, ApJ, 250, 645
Abbott, D. C., Bieging, J. H., Churchwell, E., & Torres, A. V. 1986, ApJ, 303, 239
Allen, C. W. 1973, Astrophysical Quantities (London: Athlone)
Auer, L. H., & Mihalas, D. 1972, ApJS, 24, 193
Bieging, J. H., Abbott, D. C., & Churchwell, E. 1989, ApJ, 340, 518
Blaauw, A. 1993, in Massive Stars and Their Lives in the Interstellar Medium, ed. J. Cassinelli & E. Churchwell (Provo: Brigham Young Press), 207
Blomme, R. 1990, A&A, 229, 513
Bohannan, B. 1990, in Properties of Hot Luminous Stars, ed. C. D. Garmany (Provo: Brigham Young Press), 39
Bohannan, B., Voels, S. A., Hummer, D. G., & Abbott, D. C. 1990, ApJ, 365, 729
Buscombe, W. 1969, MNRAS, 144, 1
Cassinelli, J. P. 1991, in IAU Symp. 143, Wolf-Rayet Stars and Interrelations with Other Massive Stars in Galaxies, ed. K. A. van der Hucht & B. Hidayat (Dordrecht: Kluwer), 289
Cassinelli, J. P., Waldron, W. L., Sanders, W. T., Harnden, F. R., Rosner, R., & Vaiana, G. S. 1981, ApJ, 250, 677
Castor, J. I., Abbott, D. C., & Klein, R. I. 1975, ApJ, 195, 157
Cherepashchuk, A. M. 1991, in IAU Symp. 143, Wolf-Rayet Stars and Interrelations with other Massive Stars in Galaxies, ed. K. A. van der Hucht & B. Hidayat (Dordrecht: Kluwer), 187
Chlebowski, T., & Garmany, C. D. 1991, ApJ, 368, 241
Conti, P. S. 1974, ApJ, 187, 539
Conti, P. S., & Alschuler, W. R. 1971, ApJ, 170, 325
Conti, P. S., & Frost, S. A. 1977, ApJ, 212, 728
Conti, P. S., & Niemela, V. S. 1976, ApJ, 209, L37
Cunha, K., & Lambert, D. L. 1992, ApJ, 399, 586
de Jager, C., Nieuwenhuijzen, H., & van der Hucht, K. A. 1988, A&AS, 72, 259
de Koter, A., Schmutz, W., & Lamers, H. J. G. L. M. 1993, A&A, submitted
Drew, J. E., 1989, ApJS, 71, 267
———. 1990, ApJ, 357, 573
Ebbets, D. 1981, PASP, 93, 119
———. 1982, ApJS, 48, 399
El Eid, M. F., & Hartmann, D. H. 1993, ApJ, 404, 271
Gabler, A., Gabler, R., Pauldrach, A., Puls, J., & Kudritzki, R. P. 1990, in Properties of Hot Luminous Stars, ed. C. D. Garmany (Provo: Brigham Young Press), 218
Gabler, R., Gabler, A., Kudritzki, R. P., Puls, J., & Pauldrach, A. 1989, A&A, 226, 162
Garmany, C. D., & Conti, P. S. 1984, ApJ, 284, 705
Garmany, C. D., Olson, G. L., Conti, P. S., & Van Steenberg, M. E. 1981, ApJ, 250, 660
Grevesse, N., & Anders, E. 1989, in Cosmic Abundances of Matter, ed. C. J. Waddington (New York: AIP), 1
Groenewegen, M. A. T., & Lamers, H. J. G. L. M. 1989, A&AS, 79, 359
———. 1991, A&A, 243, 429
Groenewegen, M. A. T., Lamers, H. J. G. L. M., & Pauldrach, A. W. A. 1989, A&A, 221, 78
Hamann, W.-R. 1991, in IAU Symp. 143, Wolf-Rayet Stars and Interrelations with Other Massive Stars in Galaxies, ed. K. A. van der Hucht & B. Hidayat (Dordrecht: Kluwer), 81
Hamann, W.-R., Koesterke, L., & Wessalowski, U. 1993, A&A, submitted
Harnden, F. R., Branduari, G., Elvis, M., Gorenstein, P., Grindlay, J., Pye, R., Rosner, R., Topka, K., & Vaiana, G. S. 1979, ApJ, 234, L51
Herrero, A., Kudritzki, R. P., Vilchez, J. M., Kunze, D., Butler, K., & Haser, S. 1992, A&A, 261, 209
Holweger, H. 1979, in Les éléments et leurs isotopes dans l'univers (Université de Liège), 117
Howarth, I. D., & Brown, A. B. 1991, in IAU Symp. 143, Wolf-Rayet Stars and Interrelations with Other Massive Stars in Galaxies, ed. K. A. van der Hucht & B. Hidayat (Dordrecht: Kluwer), 315
Howarth, I. D., & Prinja, R. K. 1989, ApJS, 69, 527
Humphreys, R. M. 1978, ApJS, 38, 309
Hutchings, J. B., Bianchi, L., Lamers, H. J. G. L. M., Massey, P., & Morris, S. C. 1992, ApJL, 400, L35
Klein, R. I., & Castor, J. I. 1978, ApJ, 220, 902
Kudritzki, R. P., Gabler, R., Kunze, D., Pauldrach, A. W. A., & Puls, J. 1991, in Massive Stars in Starbursts, ed. C. Leitherer, N. R. Walborn, T. M. Heckman, & C. A. Norman (Cambridge: Cambridge Univ. Press), 59
Kudritzki, R. P., Hummer, D. G., Pauldrach, A. W. A., Puls, J., Najarro, F., & Imhoff, J. 1992, A&A, 257, 655
Kudritzki, R. P., Pauldrach, A. W. A., & Puls, J. 1987, A&A, 173, 293
Kudritzki, R. P., Pauldrach, A. W. A., Puls, J., & Abbott, D. C. 1989, A&A, 219, 205
Kurucz, R. L. 1979, ApJS, 40, 1
Lamers, H. J. G. L. M. 1988, in Mass Outflows from Stars and Galactic Nuclei, ed. L. Bianchi & R. Gilmozzi (Dordrecht: Reidel), 39
Lamers, H. J. G. L. M., & de Groot, M. J. H. 1992, A&A, 257, 153
Lamers, H. J. G. L. M., & de Koter, A. 1993, A&A, submitted
Lamers, H. J. G. L. M., & Waters, L. B. F. M. 1984a, A&A, 136, 37
———. 1984b, A&A, 138, 25
Leitherer, C. 1988, ApJ, 326, 356 (L88)
Leitherer, C., & Robert, C. 1991, ApJ, 377, 629
Lucy, L. B., & Abbott, D. C. 1993, ApJ, 405, 738
Lucy, L. B., & White, R. L. 1980, ApJ, 241, 300
Maeder, A. 1990, A&AS, 84, 139
Mihalas, D. 1972, NLTE Atmospheres of B and O Stars (NCAR TN/STR-76)
Mihalas, D., & Lockwood, G. W. 1972, ApJ, 179, 829
Nugis, T. 1991, in IAU Symp. 143, Wolf-Rayet Stars and Interrelations with Other Massive Stars in Galaxies, ed. K. A. van der Hucht & B. Hidayat (Dordrecht: Kluwer), 75
Owocki, S. P. 1992, in The Atmospheres of Early-Type Stars, ed. U. Heber & C. S. Jeffery (Berlin: Springer), 393
Panagia, N., & Felli, M. 1975, A&A, 39, 1
Pauldrach, A. W. A. 1987, A&A, 183, 295

Pauldrach, A. W. A., & Puls, J. 1990, A&A, 237, 409
Pauldrach, A. W. A., Puls, J., & Kudritzki, R. P. 1986, A&A, 164, 86
Pauldrach, A. W. A., Kudritzki, R. P., Puls, J., & Butler, K. 1990, A&A, 228, 125
Peimbert, M., Torres-Peimbert, S., & Ruiz, M. T. 1992, Rev. Mex. Astron. Astrofis., submitted
Peppel, U. 1984, A&AS, 57, 107
Prinja, R. K., Barlow, M. J., & Howarth, I. D. 1990, ApJ, 361, 607
Rosendhal, J. D. 1973, ApJ, 186, 909
Schmutz, W., Hamann, W.-R., & Wessolowski, U. 1989, A&A, 210, 236
Schmutz, W., Leitherer, C., Hubeny, I., Vogel, M., Hamann, W.-R., & Wessolowski, U. 1991, ApJ, 372, 664
Scuderi, S., Bonanno, G., Di Benedetto, R., Spadaro, D., & Panagia, N. 1992, ApJ, 392, 201
Voels, S. A., Bohannan, B., Abbott, D. C., & Hummer, D. G. 1989, ApJ, 340, 1073
Walborn, N. R. 1972, AJ, 77, 312
———. 1973a, AJ, 78, 1077
———. 1973b, ApJ, 179, 517
———. 1974, ApJ, 189, 269
———. 1980, ApJS, 44, 535
Walborn, N. R., & Fitzpatrick, E. L. 1990, PASP, 102, 379
Walborn, N. R., Nichols-Bohlin, J., & Panek, R. J. 1985, *IUE* Atlas of O-Type Spectra From 1200 to 1900 Å (NASA Ref. Pub. 1155)
Wessolowski, U., Schmutz, W., & Hamann, W.-R. 1988, A&A, 194, 160
Wilson, R. 1958, Pub. Roy. Obs. Edinburgh, 2, No. 3, 61
Wright, A. E., & Barlow, M. J. 1975, MNRAS, 170, 41